

ORE LEVEL DETECTOR

Prepared For : **The Department of Electrical and
Electronic Engineering at the
University of Cape Town**

Prepared By: **Mr Michael Broek
B.Sc. Eng (Elec) UCT**

*Submitted to the University of Cape Town in partial
fulfilment of the requirements for the Degree of
Master of Science in Engineering.*

December 1989

The University of Cape Town hereby gives
the right to make copies of this thesis in whole
or in part, subject to payment of the fee by the author.

The copyright of this thesis vests in the author. No quotation from it or information derived from it is to be published without full acknowledgement of the source. The thesis is to be used for private study or non-commercial research purposes only.

Published by the University of Cape Town (UCT) in terms of the non-exclusive license granted to UCT by the author.

ACKNOWLEDGEMENTS

The author would like to thank Professor B J Downing for his supervision, assistance and encouragement during this project, and to Mr Steve Schrire for his help in the circuit design.

I would also like to thank my sister Trixie for spending endless hours deciphering my handwriting and eventually typing this thesis, and I would like to thank Van Bekkum, Leeder and Associates for the use of their word processing facilities.

DECLARATION

I declare that this thesis is my own, unaided work. It is being submitted for the degree on Master of Science in Engineering at the University of Cape Town. It has not been submitted for any degree or examination at any other university.

Signed by candidate

MICHAEL BROEK

December 1989

ABSTRACT

It was the objective of this project to design and build a transmitter/receiver unit that indicates when the ore level in a vertical ore chute falls below the level of the signal path. The design was commissioned by De Beers Consolidated Mines to be implemented in South Africa's largest diamond producing mine, the Finsch Mine at Limeacres in the north-western Cape. The system requirements laid out by de Beers stressed that the unit is to be used as a backup system, and thus its absolute reliability was of highest importance.

To monitor the correct functioning of the system, both transmitter and receiver circuitry had to be checked constantly for any possible malfunction. It was decided to include an auxiliary receiver on the transmitting side to detect the transmitted signal, thereby checking the functioning of the transmitter. On the receiving side an auxiliary transmitter unit was included that will check the correct functioning of the detection circuitry in the main receiver.

There are two ways of detecting a microwave signal. In the first, the signal is fed via a detector diode to a simple amplifying circuit. Such a detector is low in cost but has a relatively low sensitivity. An increase in sensitivity in the

order of 40dB - 50dB can be achieved using a mixer diode in conjunction with a superheterodyne receiver. However, the increase in sensitivity is traded off with an increase in complexity of the receiver circuit.

The ideal operating frequency for the unit was found in the microwave region of the electro magnetic spectrum and was chosen to be 10.35GHz. This was largely because of the commercial availability of Gunn oscillator with integral detector diode at that frequency.

The signal is required to pass through 30cm of steel reinforced concrete and 6m of air before detection. With the presence of ore the signal will be attenuated beyond detection.

The transmitter and receiver circuits forming the basis of a low cost system were designed and built. Together with the oscillator/detector module and a pair of brass horn antennas the system was tested. However, the signal strength at the receiver with the 30cm thick concrete inserted in the signal path was too weak for detection at a test distance of 6.5m. To increase the signal strength at the receiver to a level where detection can be guaranteed at all times, a transmit device operating at a power level much higher than those available by a Gunn oscillator has to be employed. However, the use of such a

device was not found viable for both practical and economic reasons. Consequently the sensitivity of the receiver had to be increased to cope with the relatively weak signal strength. A more sensitive superheterodyne receiver was designed and tested under the same conditions as the low cost system. An improvement in sensitivity of over 50dB justified its design and completed the ore level detector unit.

TABLE OF CONTENTS

	page
Acknowledgements	i
Declarations	ii
Abstract	iii
List of Illustrations	ix
<u>Chapter One</u>	
INTRODUCTION	1
1.1 The Finsch Diamond Mine	1
1.2 Ore Pass Level Measurement	3
1.3 System Requirements	4
1.4 Review of Existing Techniques	6
1.5 Choice of Approach	9
<u>Chapter Two</u>	
THE TRANSMITTER/RECEIVER UNITS	11
2.1 The IMPATT Diode	13
2.2 The Gunn Diode	16
2.3 The Gallium Arsenide Field Effect Transistor	19
2.4 The Detector	21
2.5 Considerations in Choosing the Oscillator	22

Chapter Three

DESIGN OF A LOW COST SYSTEM	25
3.1 The Self Checking Mechanism of the Level Detector Unit .	26
3.2 Description of Receiver Circuitry	29
3.2.1 The 1kHz Receiver Unit	29
3.2.2 The 1kHz and 9kHz Receiver Unit	38
3.3 Description of the Transmitter Circuitry	40
3.3.1 The Microwave Oscillator	42
3.4 Transmitter and Receiver Power Supply Circuitry	44
3.5 Antenna Design	45
3.5.1 Antenna Gain Calculations	47
3.6 The Control Box	52
3.6.1 The Decision Logic	53
3.6.2 The Main Power Supply	57

Chapter Four

PERFORMANCE OF THE LOW COST SYSTEM	60
4.1 The Receiver	60
4.2 Range Calculations	63
4.3 Range Measurements and Limitations	64
4.4 Discussion	67

Chapter Five

DESIGN OF A SUPERHETERODYNE SYSTEM 68

5.1 The Superheterodyne Principle 68

5.2 The Superheterodyne System Layout 70

5.3 The Varactor Tuned Gunn Oscillator 73

5.4 IF Amplifier and Detector Circuit Design 74

5.5 The Sweep-And-Lock Circuit Design 76

5.5.1 The Sweep System 78

5.5.2 The Sweep Window Detector 81

5.5.3 The Pause Control 83

Chapter Six

PERFORMANCE OF THE SUPERHETERODYNE SYSTEM 86

6.1 Mixer Diode Conversion Loss Measurements 86

6.2 Receiver Sensitivity Calculations 91

6.3 Signal Strength Calculations and Measurements 96

Chapter Seven

CONCLUSIONS 99

List of References 102

LIST OF ILLUSTRATIONS

	PAGE
Figure 1-1	Diagrammatic Section of the Finsch Diamond Mine . 2
Figure 1-2	Schematic Diagram of Ore Pass 3
Figure 1-3	Detailed Layout of Shaft Wall 5
Figure 1-4	Block Diagram of a Microwave Communication 8
Figure 2-1	Block Diagram of Transmitter/Receiver Unit 11
Figure 2-2	Avalanche Characteristic for a Reverse Biased P-N Junction 14
Figure 2-3	Single-drift IMPATT Diode Field Distribution and Doping Profile 15
Figure 2-4	Drift Velocity of Electrons in N-Type GaAs Versus Electric Field 17
Figure 2-5	Two Valley-Model Electron Energy Versus Wave Number for N-Type GaAs 18
Figure 2-6	Simplified Diagram of Gunn Diode 19
Figure 2-7	Schematic Diagram and Symbol of a GaAs FET 20
Figure 3-1	Schematic Diagram of the Microwave Level Detector with Transmitter and Receiver Function Check ... 27
Figure 3-2	Block Diagram of 1kHz Receiver 30

Figure 3-3	Circuit Diagram of 1kHz Receiver	33
Figure 3-4	Block Diagram of 1kHz and 9kHz Receiver	38
Figure 3-5	Circuit Diagram of 1kHz and 9kHz Receiver	39
Figure 3-6	Block Diagram of the 1kHz Transmitter	40
Figure 3-7	Circuit Diagram of the 1kHz Transmitter	41
Figure 3-8	10.35GHz Gunn Oscillator with Neighbouring Detector Diode	43
Figure 3-9	Gunn Oscillator Protection Circuit	44
Figure 3-10	Regulating Circuitry for Receivers and Transmitters	44
Figure 3-11	Horn Antenna Schematic	47
Figure 3-12	Pyramidal Horn Viewed from Waveguide End	48
Figure 3-13	Gain Reduction Factors R_E and R_H in Decibels	49
Figure 3-14	Block Diagram of the Decision Logic	54
Figure 3-15	Circuit Diagram of Decision Logic for Transmitter and Receiver Function Check	56
Figure 3-16	Circuit Diagram of Decision Logic for Ore Level Alarm	57
Figure 3-17	Main Power Supply Circuit	58
Figure 4-1	Detector Performance Test Set Up	62
Figure 4-2	Dynamic Range Compression Point	62
Figure 4-3	Block Diagram of Receiver	63

Figure 5-1	Application of Local Oscillator and Signal Voltages to a Mixer Diode	69
Figure 5-2	Block Diagram of a Simple Superheterodyne Receiver	70
Figure 5-3	Block Diagram of Proposed System	71
Figure 5-4	Outline Drawing of the Varactor Tuned Gunn Oscillator	73
Figure 5-5	Circuit Diagram of IF Amplifier and Detector ...	75
Figure 5-6	Circuit Diagram of the Sweep-and-Lock	77
Figure 5-7	Sweep System Circuit Diagram	78
Figure 5-8	Sallen and Key Type Filter	80
Figure 5-9	Sweep Window Detector Circuit	82
Figure 5-10	Section of the Pause Control Circuit	84
Figure 6-1	Mixer Spectral Diagram	86
Figure 6-2	Test Set-Up For Conversion Loss Measurement	87
Figure 6-3	Mixer Diode 1dB Compression Point	91
Figure 6-4	Receiver Block Diagram	94
Figure 6-5	Determination of Local Oscillator Power	98
Table 1	Mixer Diode Conversion Loss Fixed Input Power ..	89
Table 2	Mixer Diode Conversion Loss For Fixed IF	90

CHAPTER ONE

INTRODUCTION

1.1 The Finsch Diamond Mine

The Finsch diamond mine is the largest diamond producer in South Africa. The mine is located in the Asbestos hills near Lime Acres, a town 160km northwest of Kimberley in the Northern Cape. The orebody was first located in 1960 by Mr Fincham and Mr Schwabel whilst prospecting for asbestos. In 1963 De Beers Consolidated Mines Ltd acquired the discoverer's certificate and the planning, design and construction of a new mine began. The mine was fully established as an open pit mining operation by October 1965, with the plant treating 271 000 t/month of ore. The treatment plant was expanded in 1979-1980 increasing production to its present 420 000 t/month. However, in 1990 the open pit reaches its final economic depth of 388m and underground mining of the orebody will commence by means of a sub-level open stoping method [1].

The construction of the underground mine commenced in March 1978. Figure 1-1 below illustrates the shaft reorganization in the Finsch Mine. A 9.0m diameter main shaft was sunk to a depth of 763m and has been fully concrete lined to 743m. A 12° decline access extends from the surface to the 680m level. The

first section of the decline to the 290m level is straight and then continues as a spiral ramp, accessing each production level and the lower ground handling levels. Ore and waste will be removed from the production levels down to the 650m conveyor level via eight vertical ground passes, situated in the country rock. These passes will be developed to a diameter of 6.0m, extending from the 290m level to the 620m level. Mineral sizers will be installed below each pass on the 620m level to reduce the broken rock to pieces of about 30cm diameter, before being transported to one of the shafts by way of conveyor belts on the 650m level.

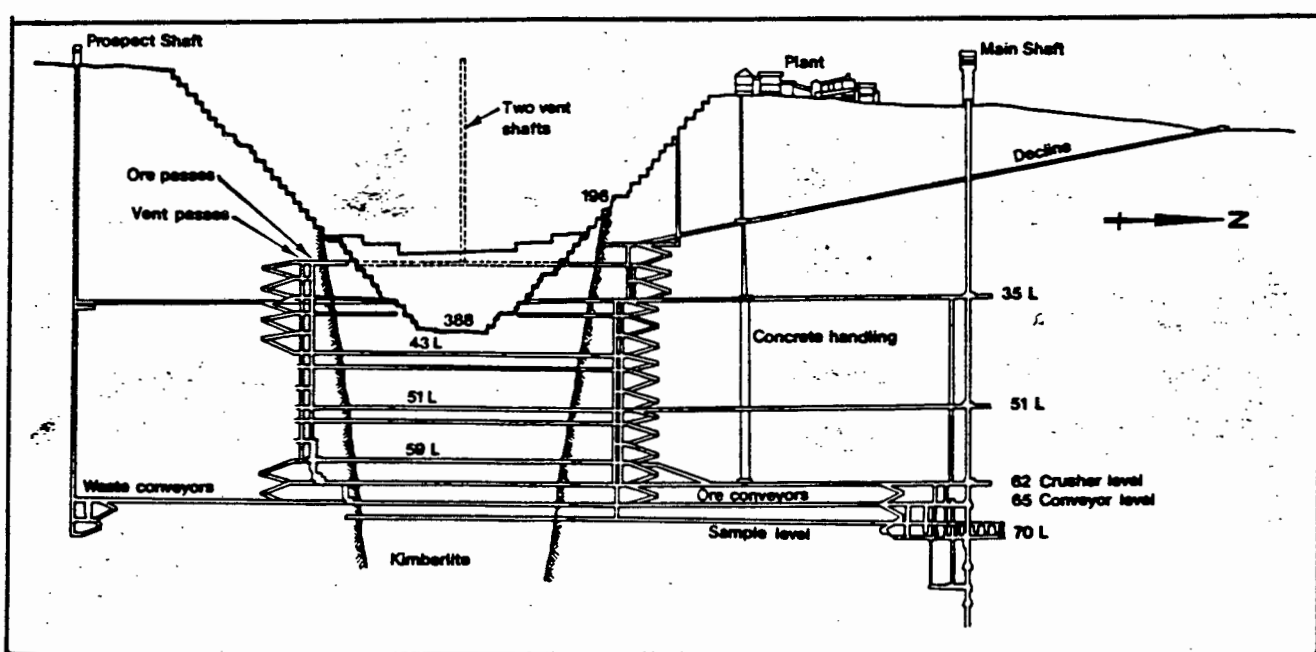


Figure 1-1 *DIAGRAMMATIC SECTION OF THE FINSCH DIAMOND MINE*

Rocks will reach the buffer at a high velocity and will then fall at a much slower rate out of the tapered end onto the provided conveyor belt. To monitor the depth of this buffer region a microwave radar system has been designed to measure the distance from the surface down to the ore level in the vertical shoot. High capital costs of both the mineral sizers and the conveyors stress the necessity of a backup system in case of a performance failure or a malfunction of the microwave radar. This backup system or ore level alarm is to detect the presence or absence of ore in the ore chute at a suitable level above the sizers.

1.3 System Requirements

De Beers Consolidated Mines commissioned this design and specified the environmental conditions under which the system is to operate. The ore level alarm is to be non-intrusive and a system consisting of a transmitter/receiver unit and mounted on either side of the shaft was proposed as illustrated in Figure 1-2. Two cavities have been provided for the mounting of the receiver and the transmitter respectively. The dimensions of these cavities were specified as 200mm x 450mm x 200mm, thus limiting the physical size of the units. Figure 1-3 gives a detailed layout of one of the shaft walls, its linings and the cavity provided.

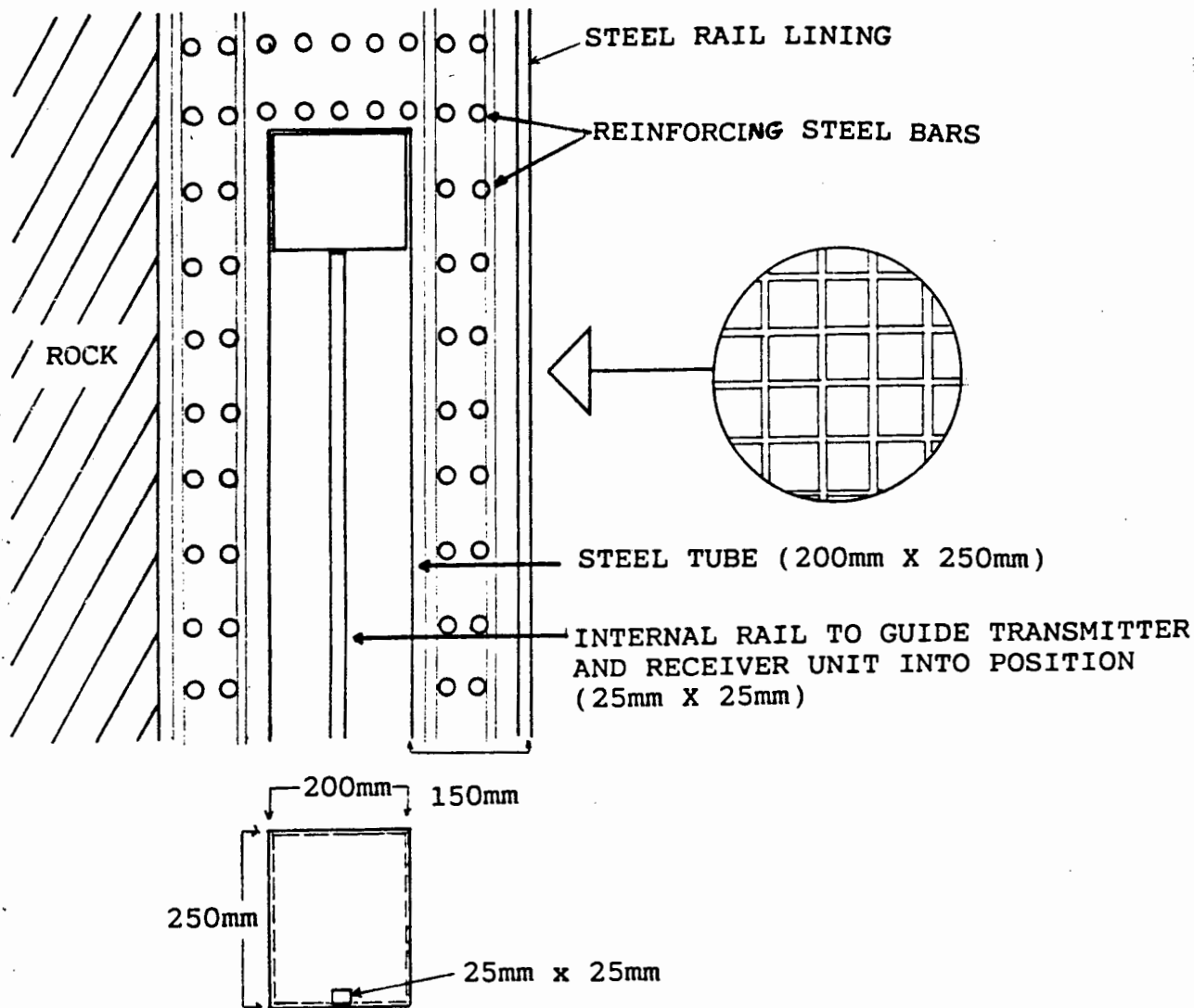


Figure 1-3 DETAILED LAYOUT OF SHAFT WALL

Since access to the units is rather cumbersome, the importance of absolute reliability of the system to rule out any further maintenance after installation has to be stressed. Once the level of the ore in the chute falls below the desired level, the unit must send an alarm message to a control box which will be situated approximately 50m from the transmitter and receiver units. This control box in turn will repeat the alarm message

to a control station on the surface. A further requirement of the system is to indicate when either the transmitter, receiver or control panel experience a power supply loss or any other kind of malfunction.

1.4 Review of Existing Techniques

A number of different techniques were considered in the design of this system and although discarded in the early stages they will find mention here.

The system requirements dictates a system consisting of a transmitter and a receiver that provide a barrier which must be broken by the ore when present. An infrared light barrier comes to mind but proves impossible to implement because of the environmental conditions imposed i.e. 15cm thick steel reinforced concrete in front of both the transmitter and the receiver. But even if the concrete were removed the falling ore would produce too much dust which is prone to collect on the devices thereby making them non-functional. Besides dust, the rocks crashing down onto each other generate a lot of noise. This noise will not lie in one particular frequency band but will contain a lot of spurious elements. Thus the choice of a transmitter/receiver unit using ultrasonics as a means of transmission was also rejected.

An electromagnetic wave link was proposed and the steel reinforced concrete and the steel rail lining around the cavities provide the biggest problem in choosing the ideal frequency.

The frequency had to be high enough to ensure propagation would occur through the gaps in the steel reinforcing bars as shown in Figure 1-3, i.e. $x > \lambda/2$ where λ is the propagation wavelength. However the frequency must be sufficiently low to allow the signal to propagate through the concrete structure without too much attenuation.

These imposed limitations narrow down the choice to a microwave communication link. The term microwave denotes that part of the electromagnetic spectrum for which the free space wavelength is between about 30cm to 3mm, covering a range of frequencies from 1GHz to 100GHz, and over. One useful characteristic of microwaves is that it becomes possible to consider radiation at such wavelengths in terms of the quasi-optical behaviour it exhibits. In Figure 1-4 below a block diagram of a simple microwave communication link is shown. Power from the transmitter is fed via a waveguide to an antenna which is designed to have directional properties appropriate to the application. The wave then propagates through free space and the energy incident on the receiving antenna will be fed to a receiver. The detection circuitry in the receiver determines

whether or not a signal has been detected and indicates this by sending an appropriate message.

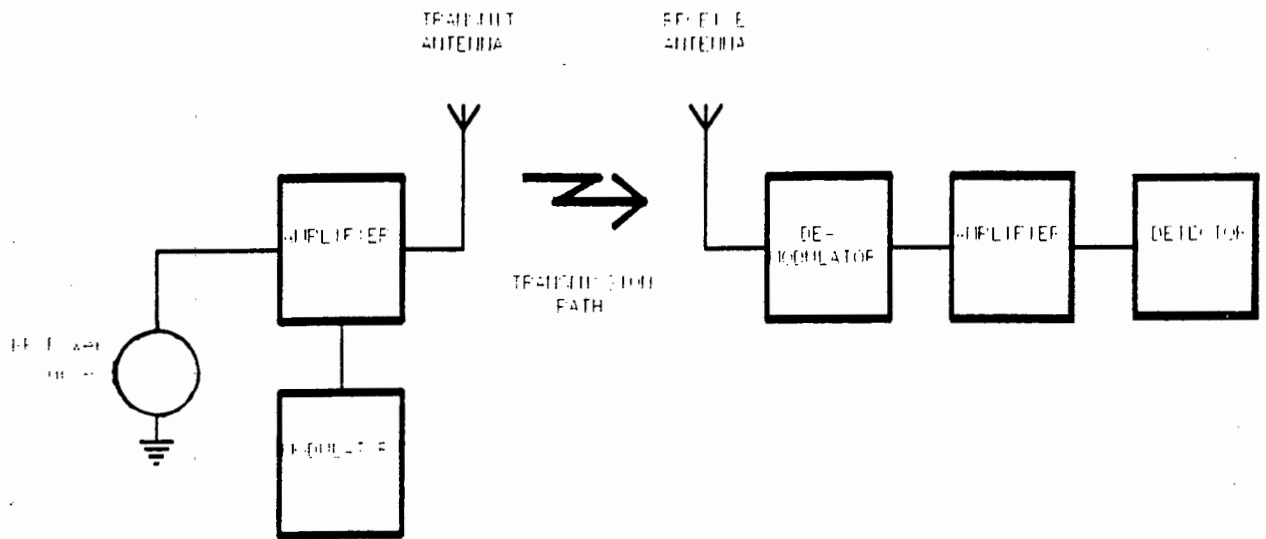


Figure 1-4 *BLOCK DIAGRAM OF A MICROWAVE COMMUNICATION LINK*

Units like the one described above are commercially available. The Nivotester FTR181 is a sophisticated non contact level detector manufactured by Endress & Hauser GmbH & Co. The transmitter and receiver are installed opposite each other and can operate over a distance of up to 20m. The system operates with a carrier frequency of 10GHz and is pulse amplitude modulated at a frequency of 1kHz. The Nivotester can generate an alarm either when the microwave beam is broken or when the propagated wave is detected by the receiver. Measurements carried out using a Hewlett Packard Network analyser at 10GHz showed that the attenuation through the 15cm steel reinforced

sections was only a few dB's. However, attenuation through the 6 metres of kimberlite rock was very high and the transmitted signal was entirely blocked from reaching the receiver. Consider an example where the transmitter malfunctions. In this case the receiver will not detect a signal whether or not the signal path is blocked. Thus it can not be determined whether there is rock present in the ore pass, or the transmitter or receiver have malfunctioned. Since the main concern of this backup system is the reliability of the error message that it generates, the commercially available unit is clearly unsuited for the use in the ore level detector.

1.5 Choice of Approach

The system requirements have been clearly layed out in Section 1.3. Summarizing, a transmitter/receiver unit is required to indicate when the ore level in a vertical ore chute falls below the signal path (safety level). To monitor the correct functioning of the system, both transmitter and receiver circuitry will have to be constantly checked for any possible malfunction. A transmitter is required to generate a wave that is to be propagated from a transmitting to a receiving antenna through a given medium. This medium consists of 15cm of steel reinforced concrete in front of both the transmitting and receiving device, and 6m of dusty air. Furthermore the wave must be able to travel through a 10cm gap between the steel

rails that line the shaft walls without showing any noticeable attenuation.

In addition the transmitted wave must be attenuated beyond detection once kimberlite rock is inserted in the signal path. The ore level alarm signal together with the transmitter and receiver function check signals are to be sent to a separated control unit. This unit will be installed in another part of the mine since the provided cavities do not allow for this bulky control circuitry to be placed within them. The purpose of the control unit is to use the incoming signals to switch one of two relays, one must be activated in case of an alarm, the other if the system experiences a malfunction.

The lower operating frequency limit of the unit is dictated by the size of the gap between the steel rails. The wavelength of the propagated wave must not be larger than twice the gap provided. This corresponds to a cut-off or lower frequency of 1.5GHz. On the other hand the propagated wave must not be attenuated to a large extent by the concrete lining of the shaft wall, giving an upper limit to the operating frequency. In this design an operating frequency of around 10.35GHz was chosen because of the commercial availability of intruder alarm oscillators in frequency band from 10GHz to 10.76GHz.

CHAPTER TWO

THE TRANSMITTER/RECEIVER UNITS

In Chapter 1 the system requirements for the ore level detector were laid out. It was concluded that both the transmitting and receiving devices have to be monitored for their correct functioning at all times. Figure 2-1 below shows a block diagram of the proposed system.

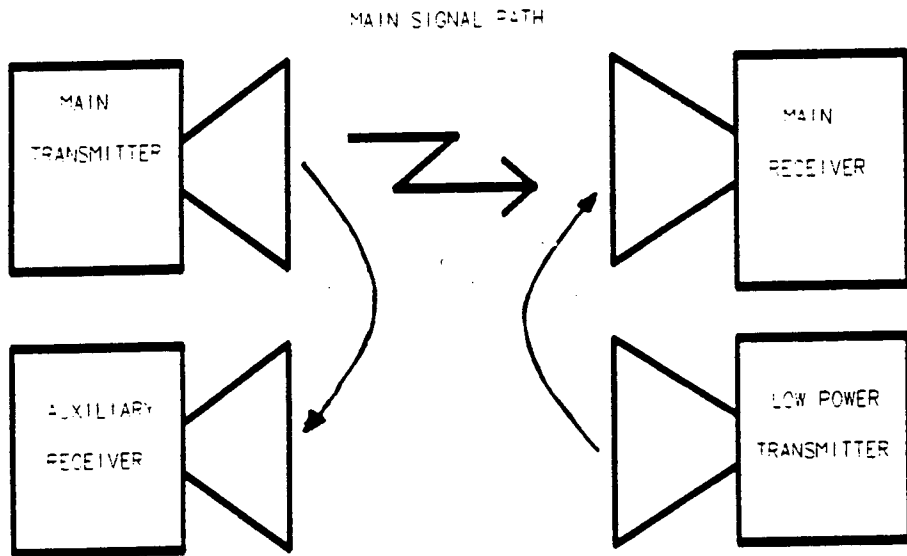


Figure 2-1 BLOCK DIAGRAM OF TRANSMITTER/RECEIVER UNIT

The main transmitter and main receiver provide the ore level detection. With the presence of ore in the signal path the microwave signal needs to be attenuated to such an extent that detection is not possible. If the transmitter is not transmitting any signal or if the detector in the receiver is

not functioning correctly, no detection will occur either. A second receiver placed next to the main transmitter will receive the transmitted signal provided the latter is operating and thus offer a function check facility for the main transmitter. The detection circuitry in the receiver will be monitored by including a low power transmitter on the receiving side of the system. This second transmitter can be a low power device since it does not have to propagate across the shaft but only to the main receiver adjacent to it. If the detection circuitry is working correctly the signal provided by the second transmitter will be detected at all times, offering a function check for the main receiver.

On the question a suitable microwave power source, a solid state oscillator was preferred to a valve source (klystron or magnetron) for the reasons of convenient power supply requirements, serviceability and reliability. These consist of two groups: (i) Three terminal devices including Gallium Arsenide microwave field effect transistor (GaAs FETs) and microwave bipolar junction transistors (BJTs) and (ii) two terminal Gunn diode and IMPATT diode oscillators.

The physical conditions imposed on the system as discussed in Chapter 1 stress the suitability of an operating frequency around 10GHz. The upper frequency limit of BJI oscillators is limited to about 4GHz and will not be considered for this

application. However they still remain a viable option below 4GHz. The most common commercially available oscillators in this frequency band are IMPATT, Gunn diode and GaAs FET oscillators. In search for a suitable oscillator for the system, these three devices will be investigated further.

2.1 The IMPATT Diode

Under certain reverse-bias conditions a P-N junction exhibits a negative AC resistance. This negative resistance can be used to sustain oscillations in a resonant circuit or to provide amplification in a reflection-type amplifier. The name IMPATT is derived from the physical mechanism involved, which are impact ionization, avalanching and transit time drift.

The possibility of such a device was originally postulated by W.T. Read of Bell Laboratories [2]. The Read diode is a basic type in the IMPATT diode family. Figure 2-2 shows the reverse bias characteristics of a P-N junction. As a result of avalanche multiplication of holes and electrons, a breakdown occurs at some voltage V_B . At this voltage electrons and holes making up the reverse current I_S gain sufficient kinetic energy to ionize further atoms on impact. This process is cumulative and the carrier density increases very rapidly. This can be seen by the steep increase in magnitude of the reverse current in Figure 2-2.

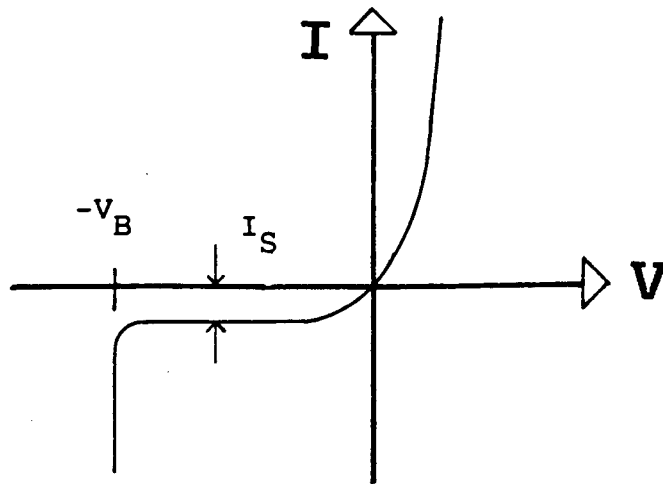


Figure 2-2 AVALANCHE CHARACTERISTIC FOR A REVERSE BIASED P-N JUNCTION

In an oscillator application the diode is biased very closely to breakdown. When connected to a resonant circuit any noise source will be sufficient to excite the circuit into oscillation. Thus the diode will swing in and out of the avalanching condition. Figure 2-3 illustrates the drift process for a $N^+ - P - I - P^+$ structure.

This type of diode is referred to as a single-drift IMPATT diode. Avalanching occurs in a narrow region close to the $N^+ - P$ junction. Electrons generated are immediately absorbed in the N^+ contact region. Hole bunches drift through the depletion region and are eventually absorbed by the P^+ contact region. The time taken for the carriers to drift from the junction to the end contacts is the transit time and thus determines the width of the drift region.

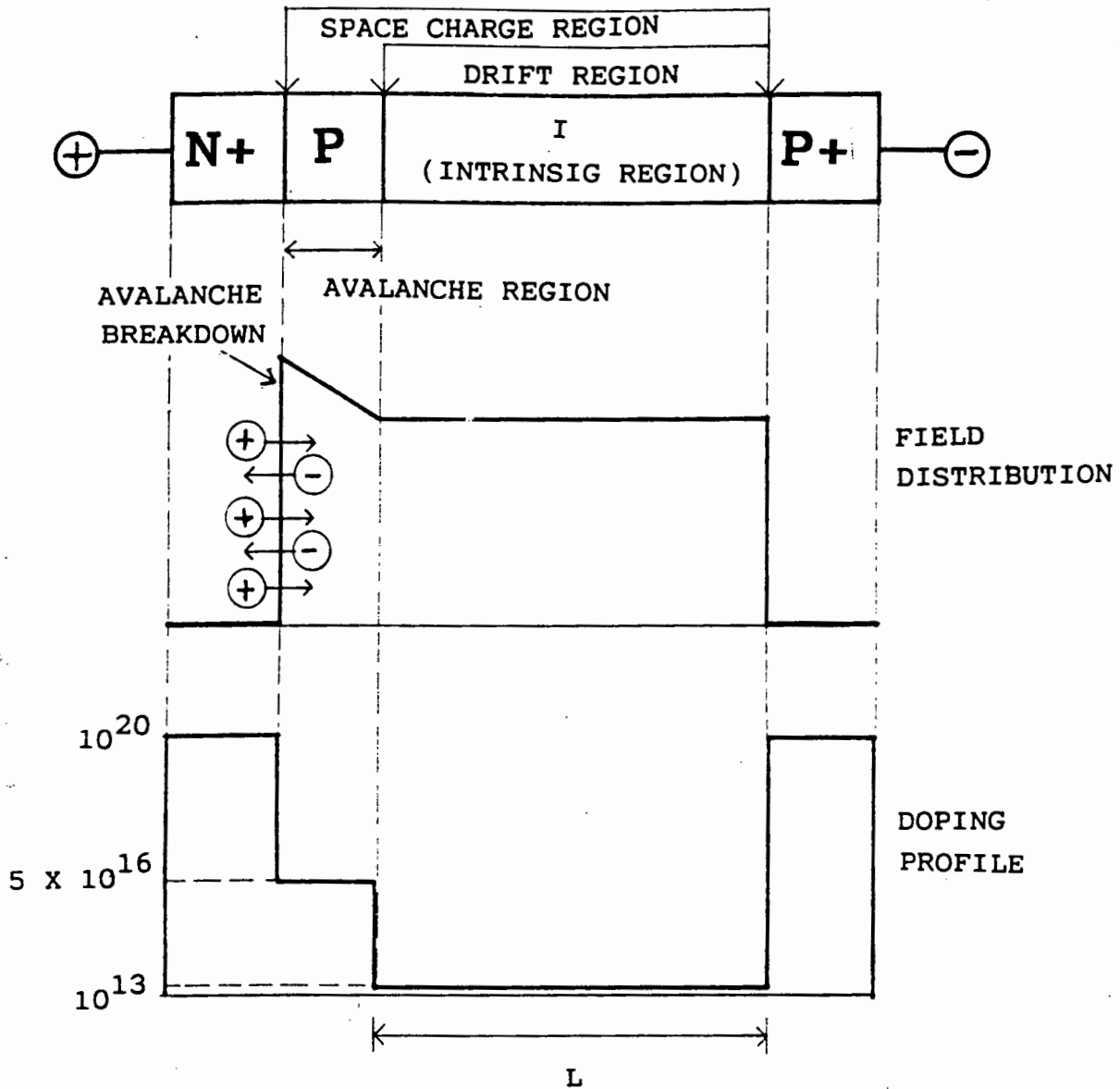


Figure 2-3 SINGLE-DRIFT IMPATT DIODE FIELD DISTRIBUTION AND DOPING PROFILE

A double-drift IMPATTs can be constructed by mounting two single drift diodes "head-to-tail", resulting in a $N^+ - I - N - P - I - P^+$ structure. Holes generated by avalanching drift in the region

to the P^+ contact and the electrons drift in the N-region to the N^+ contact. Double-drift devices provide a greater power output at better efficiency and have generally a better noise performance than single-drift devices. However they also require twice the operating voltage.

2.2 The Gunn Diode

The Gunn diode is named after J.B. Gunn who in 1963 discovered fluctuations on the current passed by both gallium arsenide (GaAs) and indium phosphide (InP) when the applied electric field exceeded a certain threshold value. In the GaAs, this fluctuation took the form of periodic oscillation superimposed upon the pulse current. The period of oscillation was found to be inversely proportional to the sample length and equal to the transit time of electrons between the electrodes. From Gunn's observation the carrier drift velocity is linearly increased from zero to a maximum when the electric field is varied from zero to the threshold of value. Beyond this value the drift velocity is decreased and the diode exhibits negative resistance. This situation is shown in Figure 2-4 on the following page.

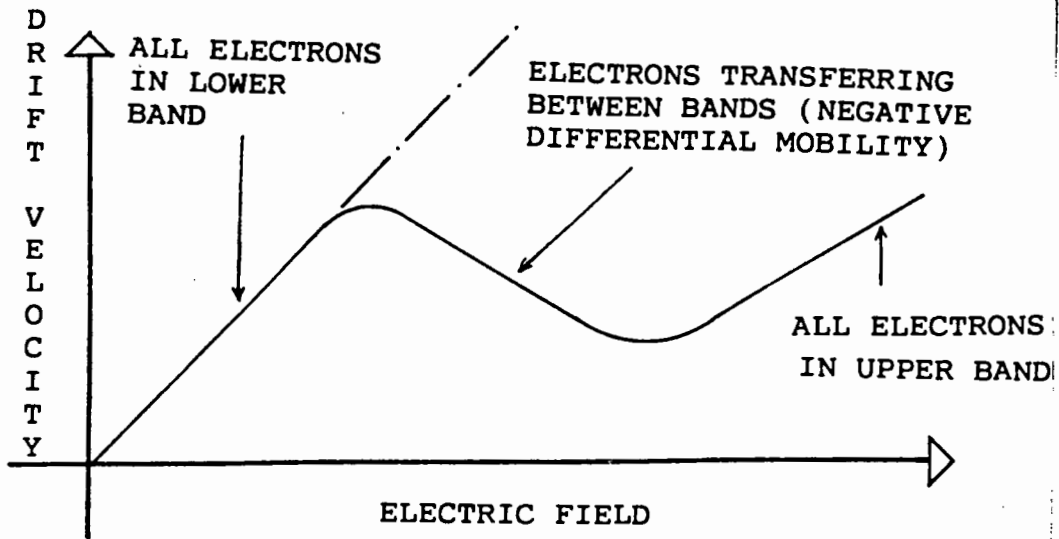


Figure 2-4 DRIFT VELOCITY OF ELECTRONS IN N-TYPE GaAs VERSUS
ELECTRIC FIELD

The principle involved is to excite electrons in a light-mass, high-mobility subband of the conduction band under the influence of an electric field so that the electrons can transfer to a heavy-mass, low mobility, higher-energy subband once they have a high enough energy. In GaAs the valleys are separated by an energy of 0.36eV as shown in Figure 2-5 [3].

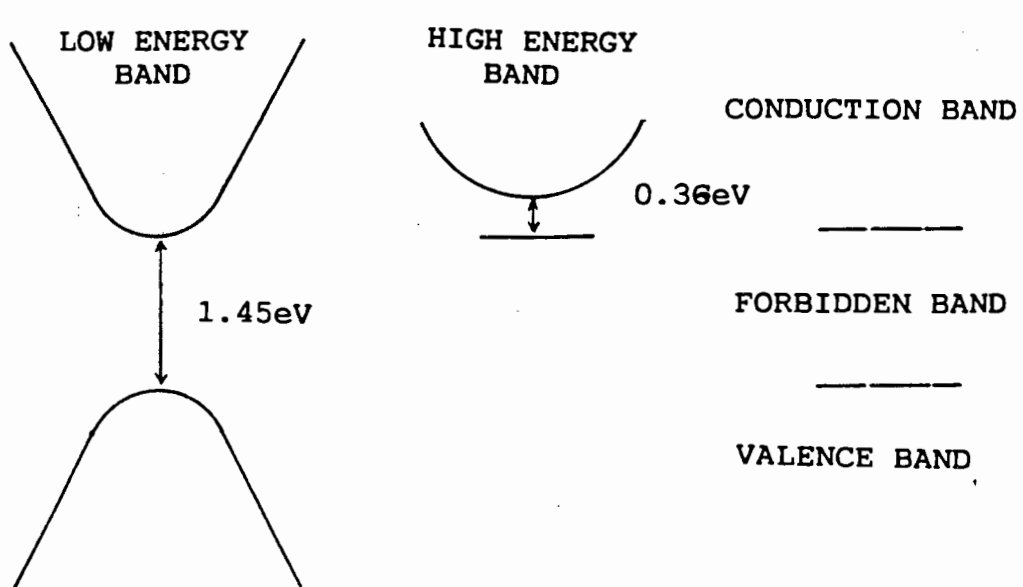


Figure 2-5 TWO VALLEY-MODEL ELECTRON ENERGY VERSUS WAVE NUMBER FOR N-TYPE GaAs

A negative differential resistivity leads to the formation of travelling domains of high electric field within the semiconductor. Since the formation of the domain reduces the field outside it, only one domain can form at a time. This mode of operation is called transit-time mode and is not very useful as its current wave form is rich in harmonics and has poor frequency stability. However by connecting an external circuit to the Gunn device, a number of sinusoidal modes of operation are possible. These are determined by the external circuit, the doping density of the device, specimen length, operating frequency and the loaded Q-factor. The most important of these is the delayed domain mode.

transistors. The type of structure used in Gallium Arsenide field effect transistors (GaAs FETs) is shown in Figure 2-7. The mobility of electrons in GaAs is about six times higher than in silicon resulting in a better high frequency performance.

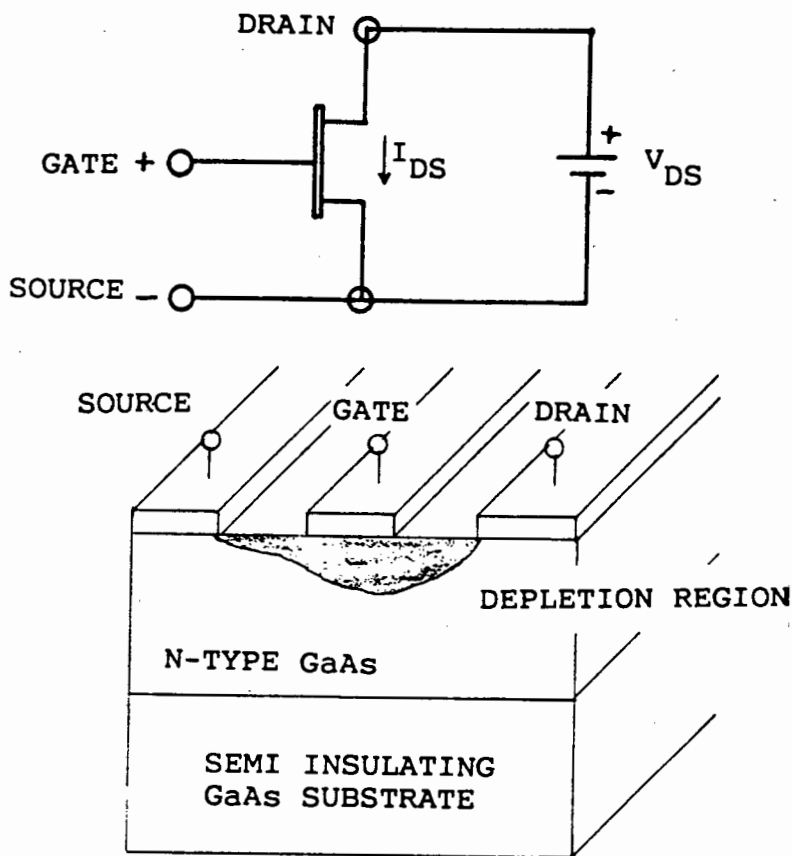


Figure 2-7 SCHEMATIC DIAGRAM AND SYMBOL OF A GaAs FET

A voltage is applied to reverse bias the schottky barrier junction between source and gate, while the source and drain is forward biased. Under these bias conditions electrons (majority carriers) move from source to drain. The current in the channel induces a voltage drop so that the gate becomes progressively more reversed-biased toward the drain. This sets up a depletion

region as indicated in Figure 2-7. As the reverse bias between source and gate increases, the depletion region increases and gradually pinches off the current through the channel. Consequently the drain current I_{DS} is modulated by the gate voltage V_{GS} [3].

2.4 The Detector

A microwave signal may be detected using (i) a detector or (ii) a mixer. In the first case, the signal is fed to a simple diode circuit. The detector diode acts as a square law detector for low level signals and can thus be used to convert low levels of amplitude modulated microwave power to modulated DC. At higher signal levels the detector will become linear and the output voltage will saturate i.e. not increase at all with increasing signals. A diode detector requires a single diode together with an impedance transformation circuit to maximize its sensitivity. Typical values vary around -45dBm. Since the output is usually at very low levels, the low frequency excess noise ("1/f noise") is a substantial part of the overall diode noise.

By using the superheterodyne principle an increase in sensitivity of the order of 40dB can be achieved. The heart of a superheterodyne receiver is a mixer diode which converts the incoming microwave to a much lower frequency at which stage

amplification is cheaper and more easily achieved. However an increase in sensitivity with the superheterodyne receive has to be traded off with the increased overall complexity of the system.

2.5 Considerations in Choosing the Oscillator

IMPATT oscillators form at present the highest power solid state device above 10GHz, giving continuous wave (CW) power of the order of several watts and peak powers of tens of watts. The upper frequency of operation is limited to about 250GHz, above which the drift region gets too thin. IMPATTs exhibit efficiencies of 10% to 15% for single drift and up to 25% for double drift devices [4]. They provide a potential reliable, compact, inexpensive and moderately efficient power source. On the other hand Gunn diodes are made at microwave frequencies ranging between 4 - 100GHz, where the upper frequency is limited by the intervalley scattering time (domain growth time) and the lower frequency limit is defined by the heatsinking capabilities of a relatively thick device. The maximum output power depends on the operating frequency and is limited to about 400mW at X-band frequency (thermally limited). Under pulsed operation the devices can have peak powers in the order of tens of watts at 10GHz. Typical efficiencies for Gunn devices vary from about 5% CW at 10GHz to up to 8% for pulsed operation at the same frequency. However, pulsed diodes are difficult to

match and have a rather limited tuning range since the bias voltages are much higher than the threshold voltages. As with the IMPATT diode, frequency drift (chirp) occurs during a pulse because of temperature rise.

One of the biggest disadvantages of the IMPATT diode is the stringent requirements of its power supply. Single drift 10GHz IMPATTs require a supply voltage of around 80V (160V for double drift IMPATT) whereas the operating voltage for a Gunn diode is only about 10V. The Gunn oscillator has a better noise performance than the equivalent IMPATT oscillator. The inherent reliability of Gunn diodes results in them being far more attractive for this application.

The frequency limitations of a GaAs FET are determined by the gate length L . The maximum frequency of oscillation f_{\max} for a GaAs FET has been found experimentally where $f_{\max} = 33 \times 10^3/L$ Hz [2]. The reflection coefficient looking into a port of the GaAs FET exhibit a linear phase change with temperature. This aids the design of oscillators with high temperature stability. At microwave frequencies the GaAs FET has a very short channel length. An increase in frequency decreases the output power (constant gain-bandwidth product). At 10GHz output powers of several watts are achieved. GaAs FET oscillators exhibit good conversion efficiencies (around 30%). However in conflict with their low noise amplifier properties the

oscillator modes appear relatively noisy. But noise figures of around 2dB make the device still viable in low noise oscillator applications.

At a frequency of 10GHz IMPATT diodes and GaAs FETs outperform Gunn devices in terms of efficiency and power output. However the difference in efficiency is not very important for this application at the frequency of interest, the main concern being the overall simplicity of the system. A market survey at this stage proved very successful in helping to choose the most suitable device. At a frequency of 10.35GHz a Gunn oscillator module with an integral detector diode is commercially available. This unit provides both an oscillator and a detector mounted inside a small waveguide cavity. Thus instead of building separate oscillator and detectors it was preferred to purchase these compact units as a basis for the ore level detector. Further, this was developed for a low cost intruder alarm application and the purchase price was only R600.

CHAPTER THREE

DESIGN OF A LOW COST SYSTEM

In section 1.5 the use of an operating frequency of around 10Ghz was justified. At this frequency the propagated wave will still be able to travel through the provided medium and emerge at the receiver relatively unattenuated. Chapter 2 stressed the advantages of using a Gunn diode as an oscillator rather than an IMPATT at the same operating frequency since the former exhibits a better noise performance. Gunn oscillators complete with an integral neighbouring detector diode are commercially available and sold as intruder alarm oscillators. The reason for using this integral transmitter/detector unit was described in Section 2.5.

It was decided to design a circuit to pulse the Gunn oscillator at a much lower frequency than the 10.35GHz. The detector thus only needs to detect this pulse frequency in order to verify the presence of the signal.

The transmitter and receiver are to be housed in two separate boxes which will be mounted inside the cavities on either side of the vertical ore chute shown in Figure 1-3. Due to the physical dimensions of the cavities, these units were designed as small as possible. Both housings are to be dust and moisture

proof, i.e. Ip 65 standard or better. Two Rose macrolon enclosures were chosen. Tests showed that the microwave signal passed through the containers unattenuated, no insertion loss was noted.

The physical size of the cavities available for the transmitter and receiver housings did not allow for a power supply unit with transformer to be mounted inside the housings. It was thus decided to power both transmitter and receiver via shielded cable from a power supply situated inside a control box. The pulsed operation of the transmitter circuit may cause voltage spikes. These in turn could be picked up by the receiver and interpreted as the actual transmitted signal. To prevent this from happening, the main power supply was designed to rectify the voltage, which is then regulated by separate regulating boards on both the transmitter and receiver side thus giving isolation between them.

3.1 The Self Checking Mechanism Of The Level Detector Unit

Under normal operating conditions the transmitted microwave signal will be attenuated by the presence of rock in the signal path to such an extent that it is not possible to detect it as a signal at the receiver. Once the level of the ore drops below the signal path, the receiver will detect the microwave signal

and transmit an alarm message to the control unit. In case of a possible malfunction of either transmitter or detector circuitry, the signal generated by the level detector will be a verification that no signal was received i.e. the alarm remains off even if the ore level drops below the signal path. For this reason it was found necessary to include transmitter and receiver function check circuitry in the design. The method found most suitable under the given conditions is described in this subsection. Figure 3-1 shows the proposed system layout.

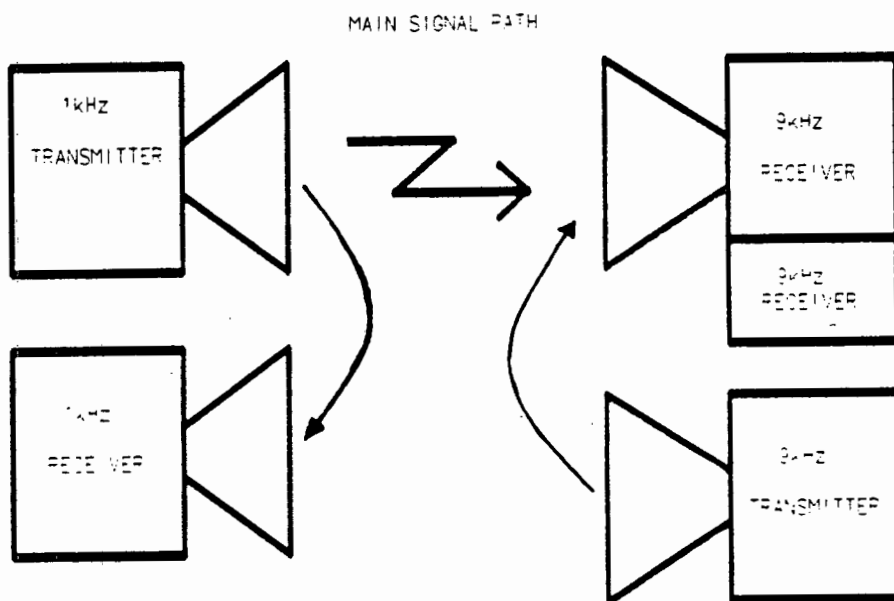


Figure 3-1 SCHEMATIC DIAGRAM OF THE MICROWAVE LEVEL
 DETECTOR WITH TRANSMITTER AND RECEIVER FUNCTION
 CHECK

To provide a check for the main transmitter an auxiliary receiver placed on the transmitting side will also detect the transmitted signal as discussed in Chapter 2. In case of a malfunction of the main transmitter, the pulsed microwave signal will not be detected by the auxiliary receiver and henceforth an error signal will be generated and sent to the control box.

The design of a function check for the main receiver unit proved to be more difficult and had to be limited to a check of the correct functioning of the detector diode. For this purpose an auxiliary transmitter placed on the receiving side transmits the 10GHz microwave signal pulsed at a frequency other than the one used by the main transmitter. A pulse frequency of 9kHz was chosen. The detector diode in the main receiver will detect both the 1kHz and the 9kHz pulse frequencies. If the detector diode is not functioning, the 9kHz pulse frequency will not be detected and consequently an error signal will be generated and then sent to the control box.

The self checking mechanism thus generates error signals when either the main transmitter or main receiver or both experience a malfunction. An error signal will also be generated if the auxiliary receiver or the auxiliary transmitter are failing to operate, since the system will believe the malfunctioning device to be the main transmitter or the main receiver.

3.2 Description Of Receiver Circuitry

To demonstrate the mechanism explained in 3.1 a model was constructed. By utilizing a frequency generator to simulate the transmitter, only the receiver circuitry had to be designed and built at this stage. Two separate boards were manufactured, one containing the main transmitter function check, the other the main receiver and the second auxiliary receiver. The design of both boards are described here.

3.2.1. The 1kHz Receiver Unit

The diagram in Figure 3-2 indicates the various building blocks that constitute the receiver circuit. The pulsed microwave signal is received by a detector diode, mounted inside a wave guide cavity which is attached to the end of the receiving antenna. The detector diode detects the envelope modulation of the incoming microwave signal. The signals at the input of a receiver are low power and accompanied by noise. Thus the output of the detector diode is first amplified and then band-pass filtered. This output is linked to the phase lock loop of a frequency/tone decoder, which locks onto a sustained frequency within its detection band. The frequency decoder in turn generates a message to be sent to a control unit.

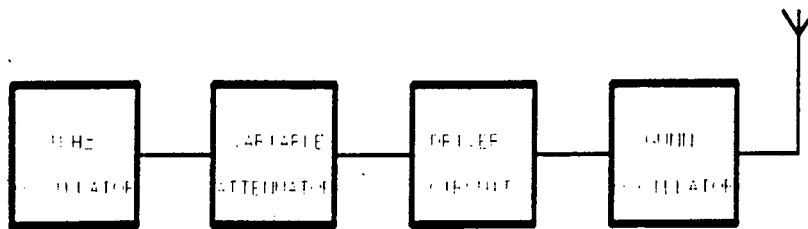


Figure 3-2 BLOCK DIAGRAM OF 1KHZ RECEIVER

A detailed circuit diagram of the 1kHz receiver is given in Figure 3-3. The output of the detector diode is AC coupled to a LM 382 low noise preamplifier (A_1) via capacitor C_1 . Capacitor C_2 sets the gain of amplifier A_1 to 40dB. The output DC voltage of amplifier A_1 is typically six volts. This allows for a good signal voltage swing. This DC offset is eliminated by an active band-pass filter centred at 1kHz, which extracts the 1kHz sinewave fundamental from the detected squarewave.

The design process of this band pass filter is described on page 287 of [5]. The bandwidth of the filter was set at 200Hz. The design of this particular filter is elaborated on the following page:

centre frequency	$f = 1\text{kHz}$
bandwidth	$BW = 200\text{Hz}$
thus quality factor	$Q = f_0/BW$
	$= 5$

angular frequency $\omega = 2\pi f_0$
 $= 6283.2$ radians/second
 and $\omega/Q = 1256.6$ radians/second

The transfer function $T(s)$ of the band pass filter is given by the following equation :

$$T(s) = k \frac{(\omega/Q) * s}{s^2 + (\omega/Q) * s + \omega^2}$$

Substitution yields

$$T(s) = \frac{1256.6 s}{s^2 + 1256.6 s + 3.95 * 10^7}$$

Now let $C_3 = C_4 = 1$ farad

and $R_1' = R_2 = R_3 = \sqrt{2} / \omega$
 $= 2.25 * 10^{-4}$ ohms

Scaling the amplitudes by 10^7 gives:

$$C_3 = C_4 = 0.1 \text{ microfarad}$$

$$R_1' = R_2 = R_3 = 2250 \text{ ohms}$$

also

$$\begin{aligned} R_6/R_5 &= 3 - (\sqrt{2}/Q) \\ &= 2.72 \end{aligned}$$

letting

$$R_5 = 1000 \text{ ohms}$$

then

$$R_6 = 2720 \text{ ohms}$$

The gain factor

$$\begin{aligned} k &= w(2\sqrt{2} - \{1/Q\}) \\ &= 16514.9 \end{aligned}$$

but the required gain is $w/Q = 1256.6$

thus introduce R_4 where $R_1' = R_1 // R_4$

$$\begin{aligned} & \frac{R_1 * R_4}{R_1 + R_4} \quad (1) \end{aligned}$$

$$\text{also } \frac{R_4}{R_1 + R_4} = \frac{\text{gain factor } k}{\text{wanted gain } w/Q} = 76.06 * 10^{-3}$$

giving

$$R_1 = 12.15 R_4 \quad (2)$$

combining (1) and (2) yields $R_4 = 2435 \text{ ohms}$ and

$$R_1 = 29588 \text{ ohms.}$$

The resistor values chosen for the band-pass filter were the closest manufactured values available and are indicated in Figure 3-3. The filter was assembled and tested. The centre frequency was found to be 995Hz with 3dB cutoff points at 885Hz and 1105Hz.

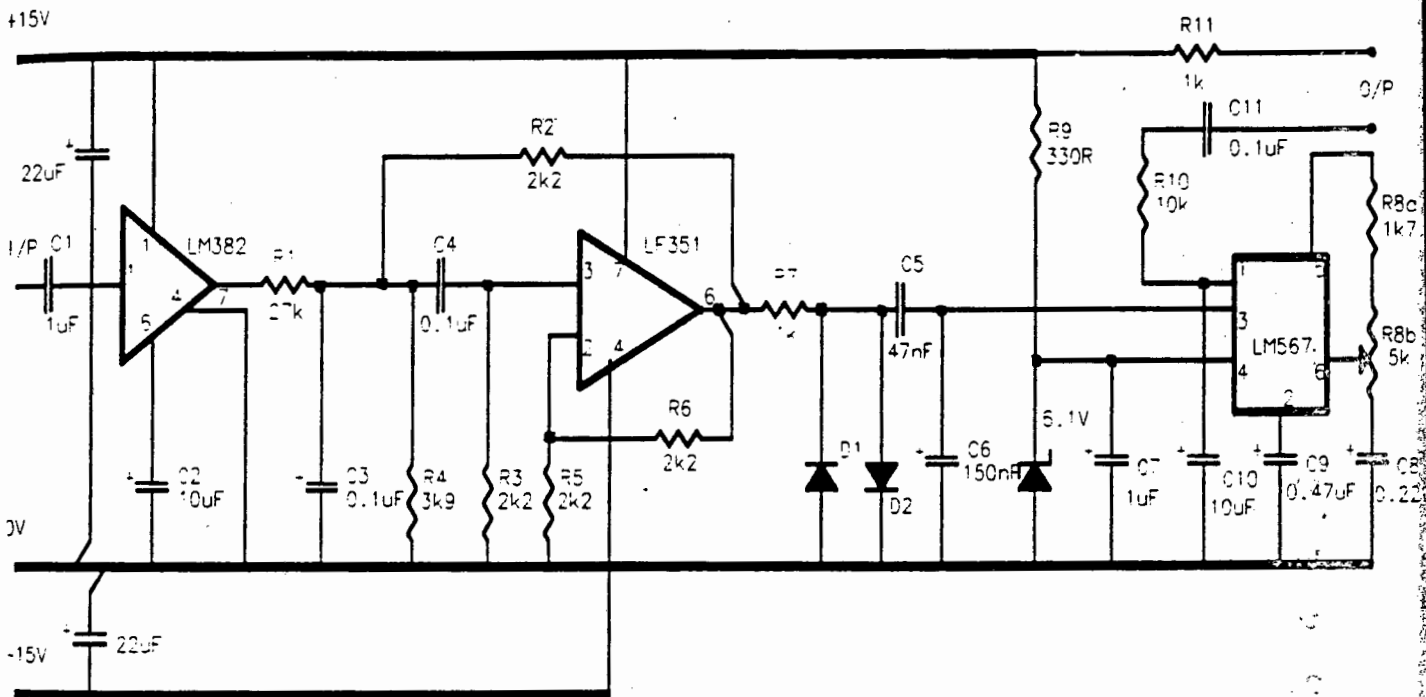


Figure 3-3 CIRCUIT DIAGRAM OF 1KHZ RECEIVER

Once the signal is band-pass filtered, a LM 567 frequency decoder will detect whether the incoming signal lies within a preset detection band.

The voltage swing at the output of the band-pass filter can be rather large (up to 13.5 volts) depending on the strength of the detected signal. However, the maximum voltage swing allowed at the input of the frequency decoder is 400 mV peak to peak. Thus the signal had to be voltage limited before entering the frequency decoder. Diodes D_1 and D_2 will limit the signal voltage down to ± 0.6 volts. Capacitors C_5 and C_6 divide the signal amplitude by a ratio of 1:3. Note that the reactance of the capacitors C_5 and C_6 at the frequency range of interest was chosen to be much less than the input impedance of the tone decoder which is 20kohms, thereby avoiding an unnecessary loading of the input of the frequency decoder. Resistor R_7 is included to limit the current into the LM 567.

The LM 567 tone and frequency decoder is a highly stable phase-locked loop. The centre frequency and bandwidth of the tone decoder can be set by the external components capacitors C_8 and C_9 and resistor R_8 . The design formulae for the LM 567 are given below:

$$\text{Centre frequency } f_0 = \frac{1}{R_8 * C_8}$$

V

$$\text{Bandwidth} \quad \text{BW} = 1070 * \frac{V}{f_o * C_9} \quad \text{in \% of } f_o, \\ V_i < 200 \text{ mVrms}$$

where V_i = input voltage in Vrms

C_9 = low pass filter capacitance in microfarad

The design procedure can be described as follows:

1. R_8 and C_8 were selected for a centre frequency of 1kHz. For good temperature stability R_8 should be between 2 kohms and 20 kohms. These values are specified by the manufacturer. To be able to tune the LM 567 at a later stage to an exact frequency, R_8 will be divided up into a potential divider R_{8a} and a series resistor R_{8b} . The series resistor is included to improve the stability of the setting.
2. Capacitor C_9 is selected for a 10% bandwidth. A 1 microfarad tantalum capacitor was chosen to improve long term stability.
3. The value of C_{10} is generally non-critical. C_{10} sets the band edge of a low pass filter which attenuates frequencies outside the detection band to eliminate spurious outputs. If C_{10} is too small, frequencies just

outside the detection band will switch the output stage on and off at the beat frequency, or the output may pulse on and off during the turn-on transient. On the other hand, if the value of C_{10} is chosen too large, turn-on and turn-off of the output stage will be delayed until the voltage on C_{10} passes the threshold voltage. C_{10} was chosen to be 10 microfarad.

4. Chatter will occur at the output when the value of C_{10} is chosen too low. This causes the output stage to move through its threshold more than once. Logic circuitry may recognize this chatter as a series of outputs. By feeding the output back to the input via capacitor C_{11} and resistor R_{10} , this chatter was eliminated.

The frequency decoder has an operating voltage range of 4.75 volts to 9 volts. For this reason the supply rail was voltage limited to a 6.1 volt Zener diode. The maximum current drawn by the tone decoder is 15mA, and the Zener diode draws approximately 4mA. By Ohm's Law the value of the resistance needed to provide enough current to both Zener diode and LM 567 can be determined, ie:

$$R_9 = \frac{15V - 6.1V}{19 * 10^{-3}A} = 468 \text{ ohms}$$

R_9 was chosen to be 330 ohms so that the I.C. is not starved of current. Capacitor C_7 decouples the Zener diode. A value of 1 microfarad was found to be sufficient.

The operation of the frequency decoder can be explained as follows. Once the centre frequency has been set, the phase-locked loop will lock whenever a frequency within its detection band is present at the input. Once locked, the output of the tone decoder will go from high to low.

The 1kHz receiver circuit in Figure 3-3 was constructed provisionally on breadboard and tested together with a frequency generator which was set to a pulse frequency of 1kHz to simulate the signal detected by the detector diode. The amplifier is limited to a maximum input signal swing of 400mV peak to peak and thus the output signal amplitude from the frequency generator had to be adjusted accordingly. With no signal present at the input of the receiver the centre frequency of the frequency decoder was tuned to 1kHz by changing the setting of the potential divider R_{8a} and observing the frequency output at pin 6 of the LM 567. By varying the input frequency to the receiver circuit the detection bandwidth was found to be 90Hz, ranging from 960Hz to 1050Hz. The function of the 1kHz receiver unit is to monitor the correct functioning of the main transmitter.

3.2.2 The 1kHz and 9kHz Receiver Unit

As discussed earlier it was decided to receive two different pulse frequencies at the receiver of the level detector, the 1kHz signal from the main transmitter and a 9kHz signal from the auxiliary transmitter. With this method the correct functioning of the detector diode can be verified. Figure 3-4 shows the block diagram of the module. After preamplification the signal is separated and fed into the 1kHz and 9kHz band-pass filters respectively. An output message is generated by each decoder and sent to the control box. This circuit is partly a duplication of the circuit described in 3.2.1.

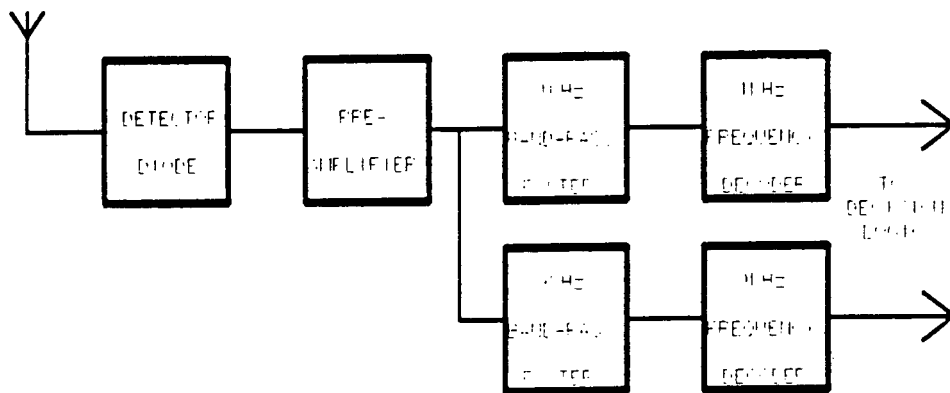


Figure 3-4 BLOCK DIAGRAM OF 1KHZ AND 9KHZ RECEIVER

A band-pass filter was designed for the 9kHz receiver using the same design procedure as for the 1kHz band-pass filter. This band-pass filter has a centre frequency of 9kHz and a bandwidth of 500Hz. A frequency decoder was set up to lock to a frequency

of 9kHz. The complete circuit diagram of this unit is shown in Figure 3-5.

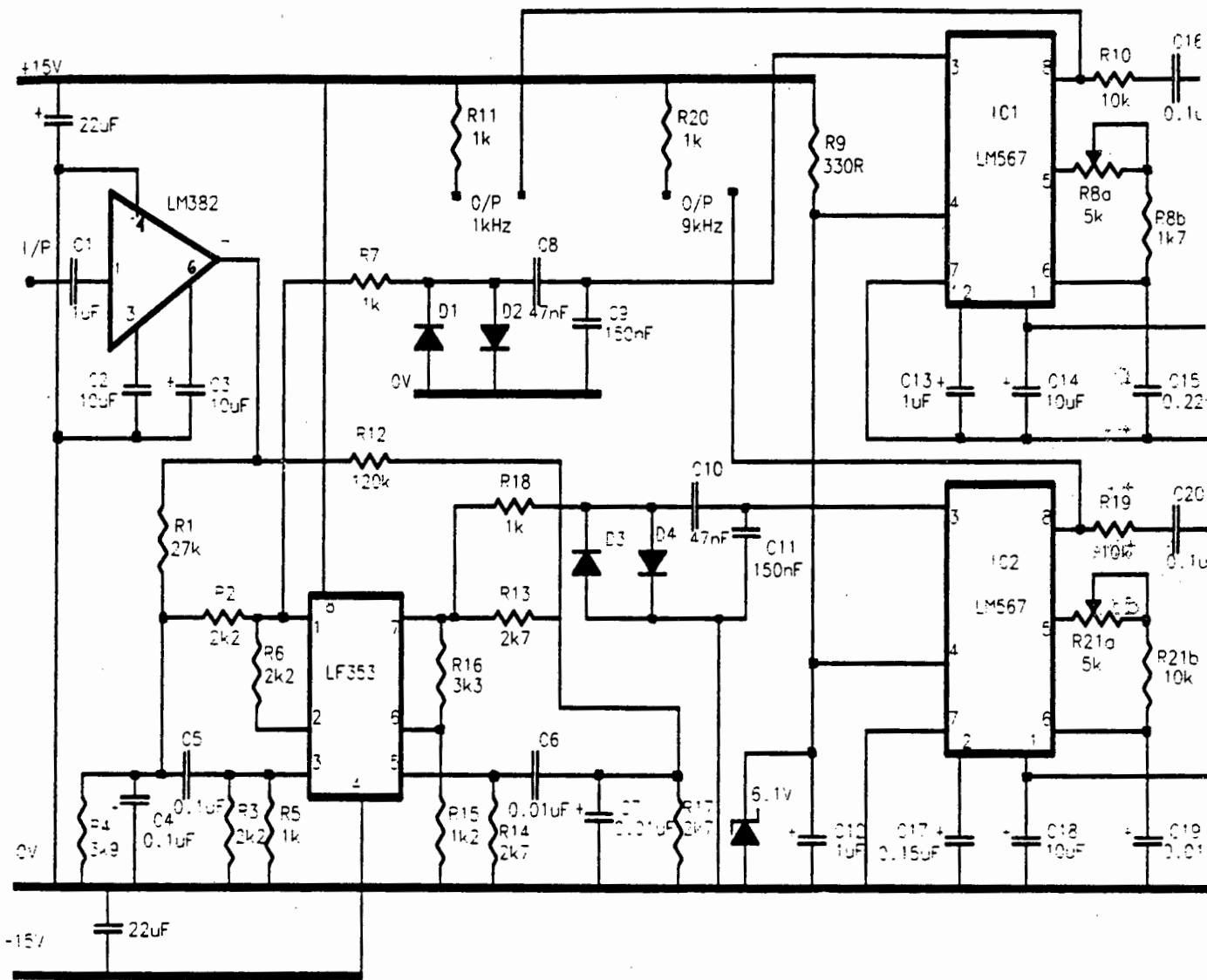


Figure 3-5 CIRCUIT DIAGRAM OF 1KHZ AND 9KHZ RECEIVER

Amplifier A₂ is a LF 353, the dual input version of amplifier A₂ used in Figure 3-3. Another notable difference between the

two circuits is that the gain of the preamplifier A_1 has been increased to 80dB by connecting capacitor C_2 from pin 3 to ground. The gain setting using external components is a feature of this preamplifier.

The circuit in Figure 3-5 was assembled on breadboard, and using the same test procedure as described in 3.2.1 its correct functioning was verified.

3.3 Description of the Transmitter Circuitry

Once the receiver circuits were built, the design of the transmitter circuit was justified. Since both the 1kHz and 9kHz transmitter are identical except for some component values, only the design of the 1kHz transmitter is explained here. A block diagram of the 1kHz transmitter is shown in Figure 3-6.

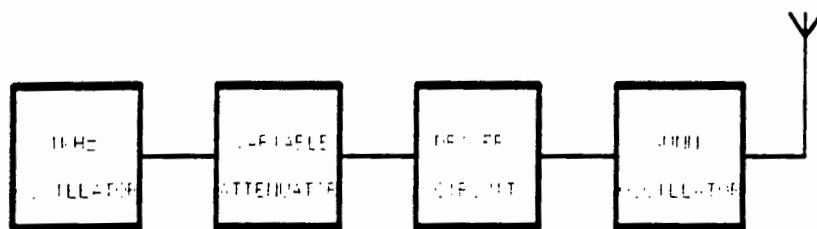


Figure 3-6 BLOCK DIAGRAM OF THE 1KHZ TRANSMITTER

The 1kHz oscillator is followed by a tuneable voltage attenuator. This allows different microwave sources to be driven by the same circuit. The attenuator is coupled to a driver circuit which in turn drives a Gunn oscillator module.

The complete circuit diagram of the 1kHz transmitter is shown in Figure 3-7. A LM 555 timer is used to provide an oscillation frequency of 1kHz. The frequency of oscillation is dictated by the ratio of the resistances R_1 and R_2 and the capacitor C_1 in the equation below [6]:

1

$$\text{frequency of oscillation} = \frac{1}{0.693 * (R_1 + 2 * R_2) * C_1}$$

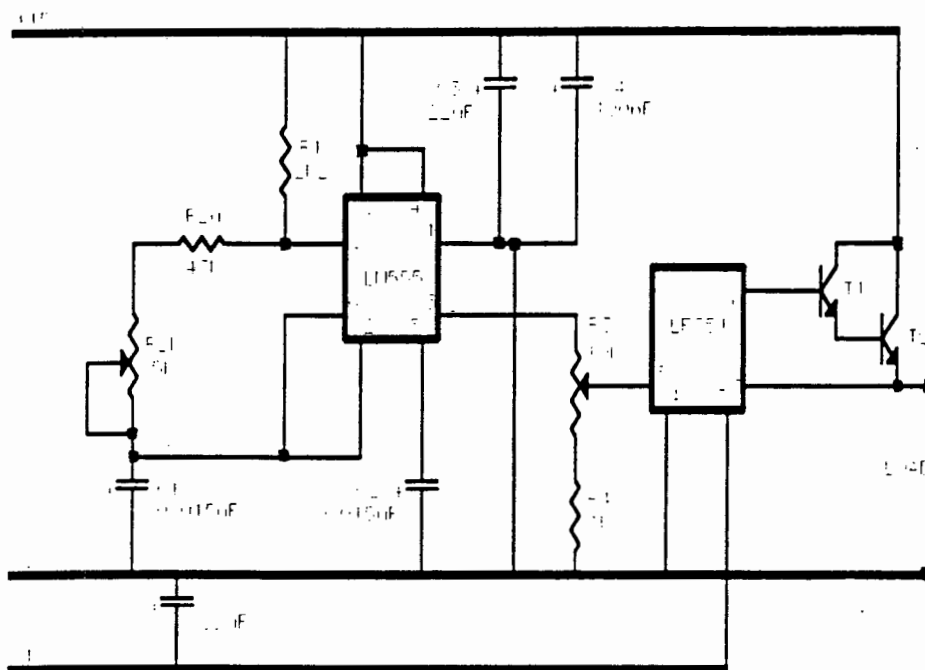


Figure 3-7 CIRCUIT DIAGRAM OF THE 1KHZ TRANSMITTER

The values chosen for C_1 and R_1 were 0.015 microfarad and 2200 ohms respectively. R_2 was then divided into a 47kohm resistor and a 5kohm potential divider. This configuration facilitates a tuning of the oscillation frequency. In the 9kHz

transmitter circuit these three components have the following values:

$$C_1 = 0.015 \text{ microfarad}$$

$$R_1 = 1000 \text{ ohms}$$

$$R_2 = 3900 \text{ ohms and a } 1000 \text{ ohms potential divider}$$

Capacitors C_3 and C_4 are power supply decoupling capacitors. C_3 is included for smoothing and C_4 to filter any high frequency spikes that might occur.

The output of the LM 555 is coupled to an attenuator R_3 . A series resistor R_4 is included to improve the stability of the voltage attenuator. The output of the attenuator is fed to the non-inverting input of amplifier A_1 . Amplifier A_1 is a LF 351 op-amp and is configured as a follower. It drives the base of the small signal transistor T_1 . T_1 and the power transistor T_2 are connected in a Darlington configuration. This configuration can deliver an output current of more than two amps which is more than enough current to drive the oscillator. The oscillator is connected between the emitter of T_2 and ground.

3.3.1 The Microwave Oscillator

The microwave oscillator used is a commercially available 10.35GHz intruder alarm Gunn oscillator with neighbouring or

integral detector diode. This device is shown in Figure 3-8.

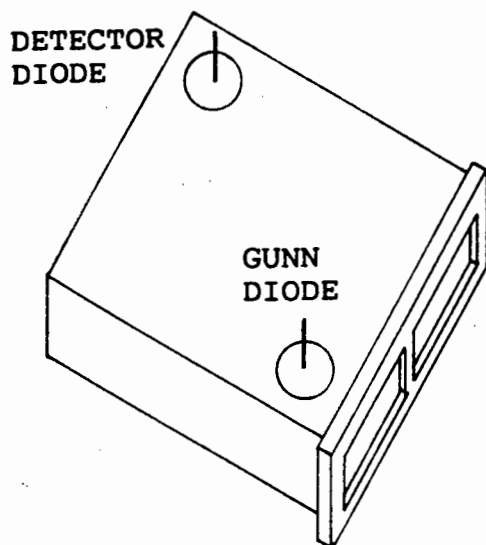


Figure 3-8 10.35GHZ GUNN OSCILLATOR WITH NEIGHBOURING
DETECTOR DIODE

The oscillator requires a supply voltage of 7 volts and draws a maximum current of 150mA. The transmit power of the oscillator is 8.5mW. A 7.1 volt zener diode is connected across the Gunn oscillator to prevent it from being damaged by supply voltage spikes and a 1N4198 diode is used to protect it from becoming reverse biased when the supply is switched off.

To improve the stability of the circuit a 0.1 microfarad capacitor is connected across the oscillator terminals. All three components were mounted directly to the oscillator terminals. Figure 3-9 below, gives a schematic diagram of the oscillator protection circuitry.

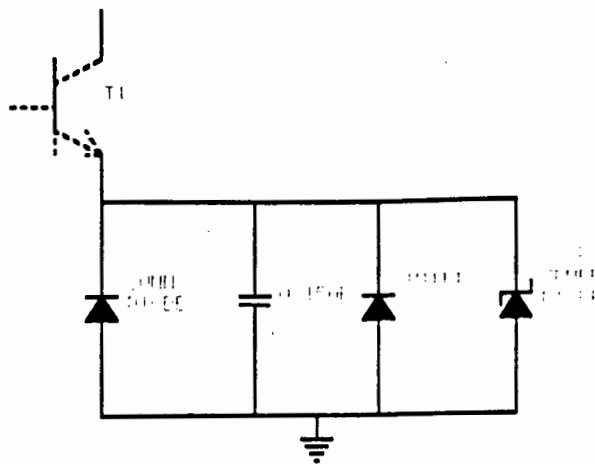


Figure 3-9 GUNN OSCILLATOR PROTECTION CIRCUIT

3.4 Transmitter And Receiver Power Supply Circuitry

It was decided to provide the transmitters and receivers with a rectified voltage from an external supply. Thus regulating circuitry had to be included on the transmitter and receiver boards. The circuit diagram of the regulating circuit is shown in Figure 3-10.

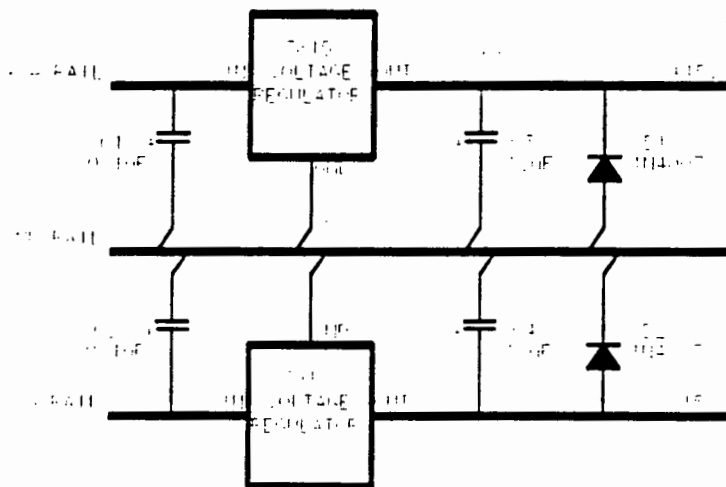


Figure 3-10 REGULATING CIRCUITRY FOR RECEIVERS AND TRANSMITTERS

Capacitors C_1 and C_2 filter out high frequency noise that might appear on the supply rails. The positive and negative rails from the rectifier are connected to the 7815 and the 7915 voltage regulator. The voltage regulators provide a stable +15 volt and -15 volt supply rail. When mounted in a sufficient heat sink, they can source an output current of up to 1.5 A each. C_3 and C_4 are 10 microfarad tantalum capacitors and provide further smoothing of the 15 volt dc rails. Diodes D_1 and D_2 provide output short circuit protection.

The above regulating unit was added to each of the transmitter and receiver circuits. The layout of the circuit was designed on an IBM compatible Personal Computer using the software draughting package Smartwork. All the circuits described above were built on printed circuit board and tested for their correct functioning.

3.5 ANTENNA DESIGN

The part of a microwave system that involves the launching of a beam of electromagnetic radiation by an antenna, the propagation of the beam and subsequent reception is central to the performance of the system. An antenna is used to transfer energy to and from space. In this process energy is dissipated as heat in the structure of the antenna. Since there are a host of other sources of loss which are more difficult to identify, the determination of efficiency of an antenna depends on being

able to measure total power input and total power radiated. It is also important to note that for a given antenna the efficiency is the same for transmit and receive modes of operation. In the present design the energy from the Gunn diode module needs to be propagated into space. The electromagnetic energy of the Gunn diode could be transmitted and received through the open end of the waveguide cavity. However, this is a very inefficient way of coupling a waveguide to space, as a sudden change in cross section area results in reflections. This impedance mismatch at the mouth of the module can be improved by flaring out the sides into a horn, thereby producing impedance match between the waveguide and the intrinsic impedance of free space [7]. Horns flared in both E and H plane are called pyramidal horns. The design and manufacture of such pyramidal horns is relatively simple and was thus found to be the obvious choice for transmit and receive antennas.

The only limitation of physical dimension of the pyramidal horn is the size of the aperture. The larger the aperture, the larger is the directivity of the antenna, but the phase distribution across the aperture becomes also greater. To prevent any phase distortion from occurring, the length of the walls of the horn are limited to the length of the horn plus approximately 60° or a sixth of the wavelength of the transmit frequency. This limitation is reflected schematically in Figure 3-11 on the following page.

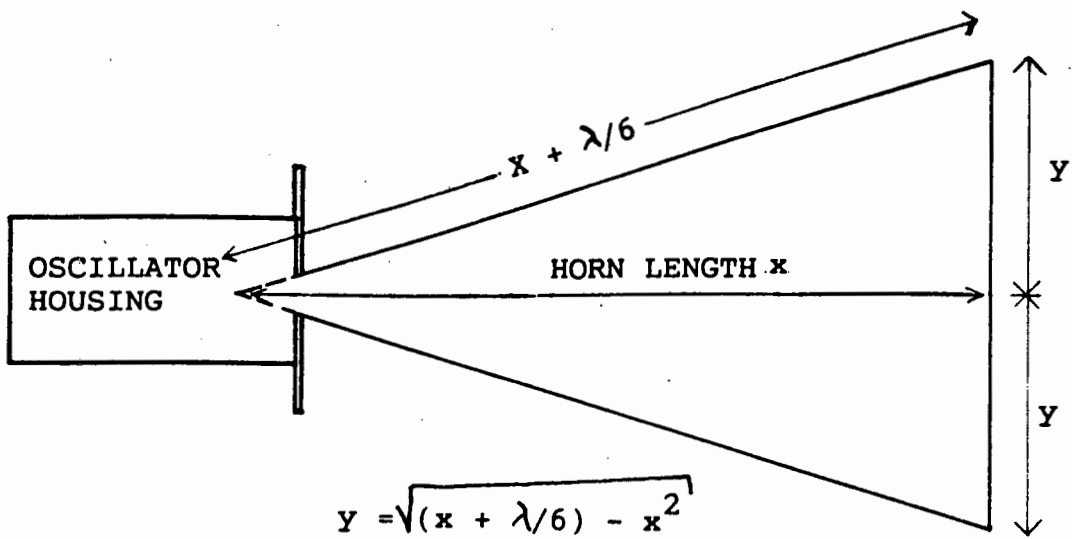


Figure 3-11 HORN ANTENNA SCHEMATIC

The physical size of the transmitter and receiver housings limited the length of the horns to 10cm. At a frequency of 10.35GHz, the wavelength is equal to 2.84cm. The value of y in Figure 23 was calculated as 3.12cm. In order not to make the design too critical the aperture size was chosen to be 6cm, slightly less than twice the value of y.

Horn antennas were fabricated and tested and were shown to operate satisfactorily.

3.5.1 Antenna Gain Calculations

The gain of a horn antenna depends on the wavelength, the aperture dimensions a and b and the slant length l_E and l_H . Figure 3-12 shows the dimension of the pyramidal horn used.

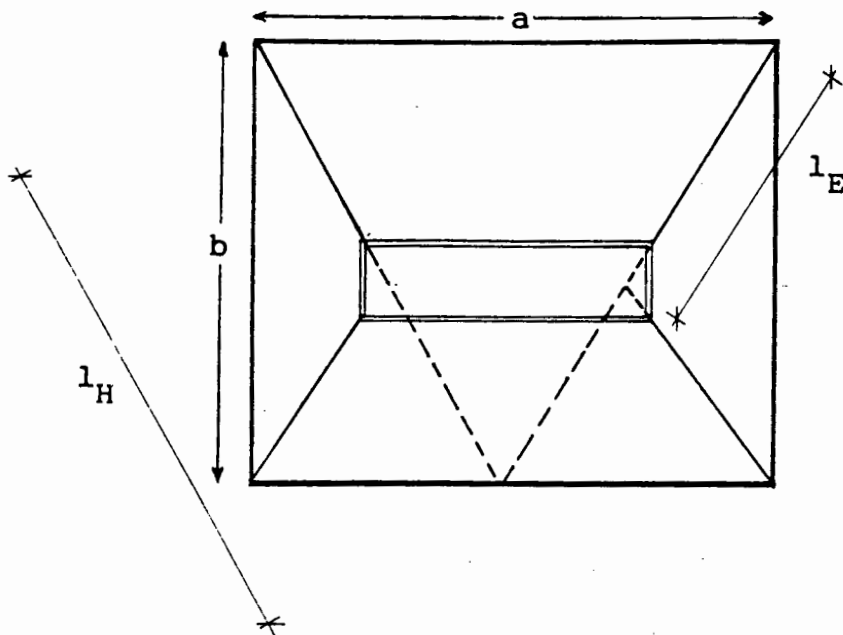


Figure 3-12 PYRAMIDAL HORN VIEWED FROM WAVEGUIDE END

The isotropic power gain G for the antenna is given as [8]

$$G = G_0 R_E R_H$$

where R_E and R_H are the gain reduction factors which take into account the E and H-plane flare of the horn. The values for R_E and R_H are presented graphically in Figure 3-13.

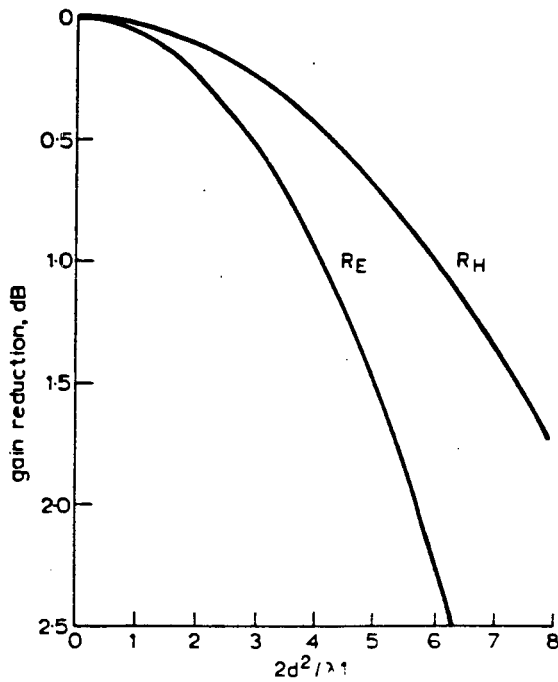


Figure 3-13 GAIN REDUCTION FACTORS R_E AND R_H IN DECIBELS

When using the above to determine the value of R_E , it is necessary to substitute the value of a for d and l'_E for l (to determine R_H substitute b and l'_H). The parameters l'_E take the range and slant heights into account and can be calculated as follows [8]:

$$l'_E = \frac{r * l_E}{r + l_E}$$

$$l'_H = \frac{r * l_H}{r + l_H}$$

The characteristics of importance in the present application concern the farfield, which is taken as the region beyond a radius of $2D^2/\lambda$ centred at the antenna, where λ is the free space wavelength and D the length of the antenna aperture.

For the farfield gain, $l_E = l'_E$ and $l_H = l'_H$. A further simplification can be achieved by noting that the slant lengths have equal magnitudes ($l_E = l_H = l$) and that $a = b = d$. The abscissa values in Figure 27 are then

$$S = \frac{2d^2}{\lambda l}$$

From the same Figure we then get $R_H = -0.45\text{dB}$ and

$$R_H = -0.25\text{dB}.$$

The value of G_0 can be obtained by evaluating the following expression:

$$G_o = \frac{32d^2}{\lambda^2\pi}$$

and works out to be 16.37dB. The overall antenna gain in dB is then $G = 16.37 - 0.45 - 0.25 = 15.67$ dB, with a beamwidth of nominally $\lambda/d = 28.5^\circ$.

The radiation pattern of an antenna defines its directional properties and is basically a function of the field distribution within the aperture. For a particular horn aperture the directivity is greatest when the field distribution is uniform. Variations of field intensity across the aperture will have the effect of skewing the polar diagram, reducing the directivity and increasing the sidelobe levels. The antenna gain is defined at the maximum of the radiation pattern compared to an isotropic radiator. It must be noted that it is only a gain in the sense that the antenna concentrates or focuses the power in this direction, it does not increase the total power radiated.

In reception the input port is connected to a load and of concern is the amount of power absorbed by the antenna from the radiation falling on it. The power delivered by an antenna to a load appears to come from a source of internal impedance equal to the radiation impedance of the antenna, R_a and jX_a where the resistive component R_a is the representation of the power

lost to the source by radiation and the reactance X_a represents energy stored in the near field of the antenna. A waveguide horn antenna however is better characterized in terms of its reflection coefficient. Thus in wave terms the source has the same reflection coefficient as the antenna has in transmission.

3.6 The Control Box

The circuitry described so far is housed in the two boxes, mounted inside the cavities on either side of the vertical ore chute. The boxes provide three outputs: the low level alarm, the transmitter function check and the receiver function check. These messages have to be interpreted and sent to a control room in the Finsch mine, where the necessary actions will be taken. To provide a link between the receiver outputs and the control room, an interface was designed using two relays. One relay is activated when the ore level in the chute drops below the signal path, the other when either transmitter or receiver experience a malfunction. The power supplies for the transmitters, receivers and the logic circuits is also placed inside the control box. The design of the decision logic circuits and the power supply circuit is discussed here.

3.6.1 The Decision Logic

The output of the receiver circuit is taken from pin 8 of the frequency decoder. This output is either a logical 0, i.e. the ground rail, or a logical 1, i.e. the 6.1 volt supply rail of the frequency decoder. These signals are linked to the control box via 50m of shielded cable. The resistance of this cable was measured to be 2.5 ohms since the current consumption of the transmitter/receiver units is less than 600 mA, the voltage drop that will be experienced along the shielded cable can be evaluated using ohm's law and turns out to be 1.5 volts. This voltage drop might cause a problem if the receiver outputs are linked directly to the decision logic.

To circumvent this problem a MGT 6 optoisolator was used. Each channel of the optoisolator consists of an NPN silicon planar phototransistor optically coupled to a gallium arsenide infrared emitting diode. The function of the MCT 6 is thus to isolate floating grounds and voltage transients that might occur along the transmission line.

Figure 3-14 shows a block diagram of the decision logic. It can be seen that the decision logic consists of the optoisolator followed by a logic circuit. The logic output is coupled to a current driving stage which in turn switches a relay. The normally open contacts of the relay are used in an external circuit to drive an alarm system in the control room.

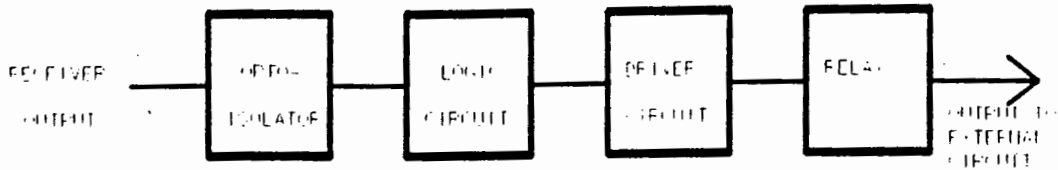


Figure 3-14 BLOCK DIAGRAM OF THE DECISION LOGIC

A complete circuit diagram of the decision logic for the transmitter and receiver function check is shown in Figure 3-15. The two 1kHz resistors at the input of the optoisolator are mounted on the respective receiver circuit boards (R_{11} in Figure 3-3 and R_{20} in Figure 3-5). They are used as a short circuit protection for the power supply. Their values were chosen to provide enough current to the light emitting diodes D_1 and D_2 .

Pins 2 and 3 of the MCT 6 are connected to the outputs of the 1kHz auxiliary receiver and the 9 kHz auxiliary receiver. When the signal of either of these outputs goes high, i.e. indicating a malfunction of either device, the infrared emitting diode will stop conducting. This forces the phototransistor to switch off. Its output is then pulled high via R_1 or R_2 .

The MC14093B Schmitt trigger Nand gate is configured in such a way that if either pin 6 or pin 8 of the MCT 6 goes high pin 11 of the Nand gate will also go high. This signal is then used to switch the relay.

To prevent voltage transients from causing false alarms, a RC time delay was arranged. R_3 and C_1 were chosen to give a delay of about 5 seconds, i.e. only if a high output from the Nand gate is sustained for at least 5 seconds, the relay will be switched into conduction. Diode D_3 allows a quick discharge of capacitor C_1 .

The driving stage consists of small signal transistor T_1 and power transistor T_2 connected in a Darlington configuration. Diode D_4 serves as a protection for the Darlington configuration. When the transistor is on, i.e. when the relay is switched on, D_4 is reverse biased. When the transistors are switched off, the current in the inductive coil of the relay cannot turn off suddenly since that would imply an infinite voltage across the terminals of the relay. Instead the voltage across the inductor suddenly rises and keeps on rising until it forces current to flow. Since the transistors cannot withstand the inductor's craving for current, it would eventually break down if D_4 was not connected across the relay terminals. Thus at turn-off the diode goes into conduction thereby putting the switch terminal a diode voltage drop above the 15 volt rail.

The functioning of the decision logic for the low level alarm is practically identical. A diagram of this circuit is shown in Figure 3-16. The input to pin 2 of the optoisolator comes from the main 1kHz receiver. Note that this circuit energizes the relay coil when the input to the circuit is low, i.e. when the frequency decoder has locked.

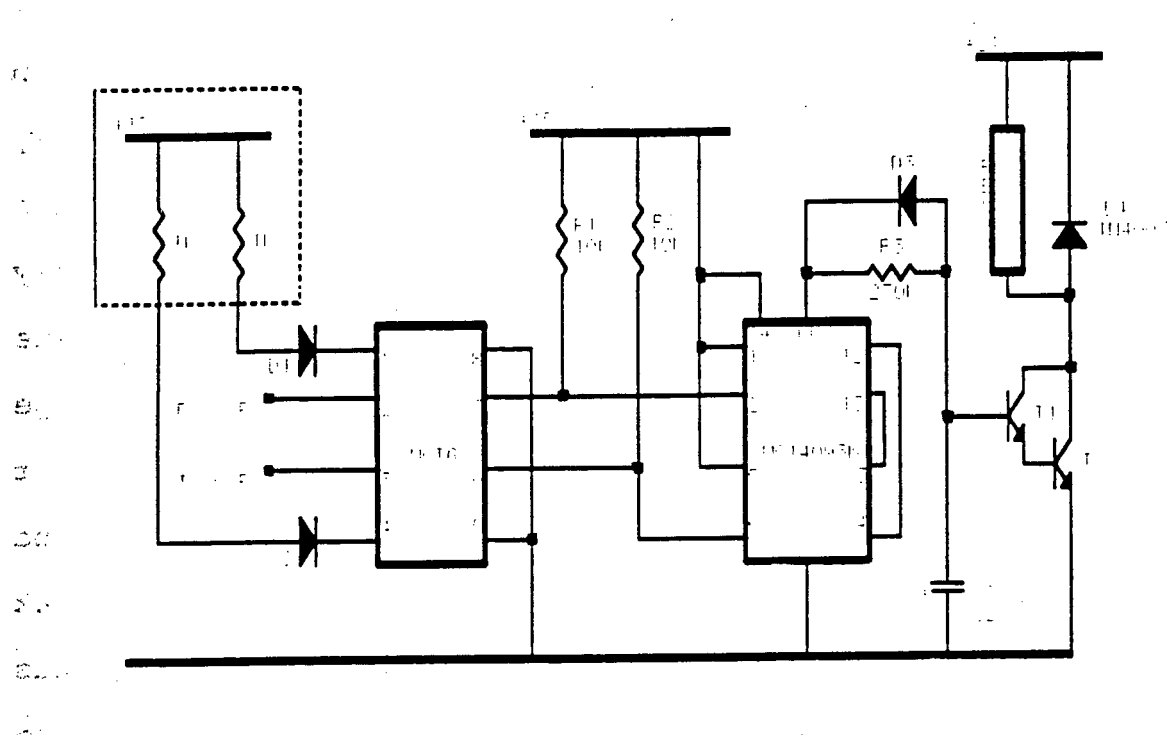


Figure 3-15 *CIRCUIT DIAGRAM OF DECISION LOGIC FOR TRANSMITTER AND RECEIVER FUNCTION CHECK*

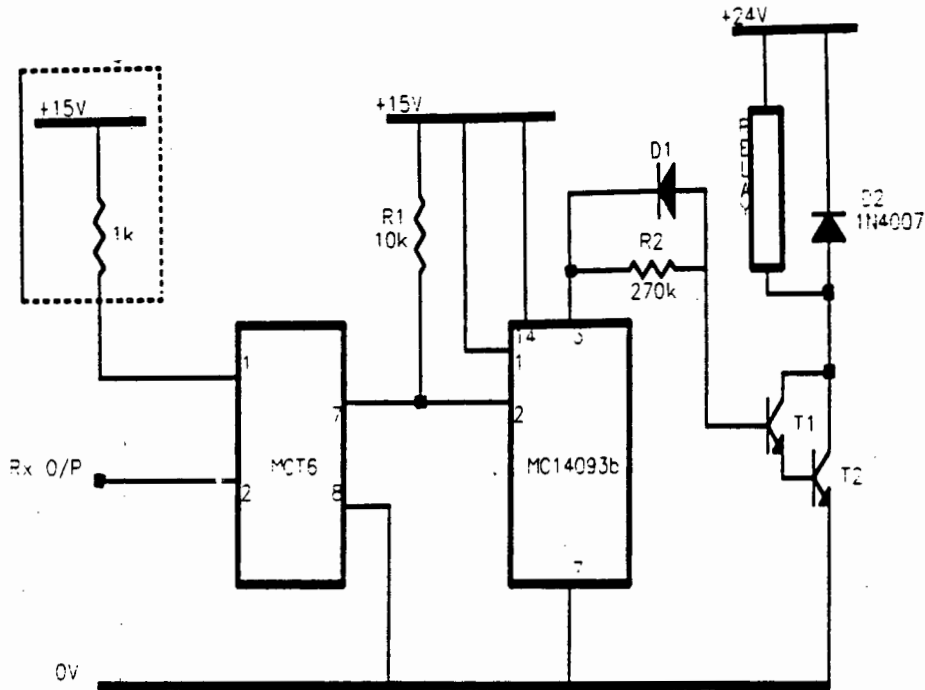


Figure 3-16 *CIRCUIT DIAGRAM OF DECISION LOGIC FOR ORE LEVEL ALARM*

3.6.2 The Main Power Supply

The transmitter and receiver circuits described in this chapter require a ground rail and positive and negative recessed voltage rails of about 20 volts each. The decision logic circuits require regulated +15 V and 0V supply rails. The relays need rectified 24 volts for correct operation. The circuit diagram of the main power supply is shown in Figure 3-17. A transformer was wound to run of both 110 volts ac and 220 volts AC, thus making it possible to use the transformer for both testing in the laboratory and for the installation in the Finsch mine.

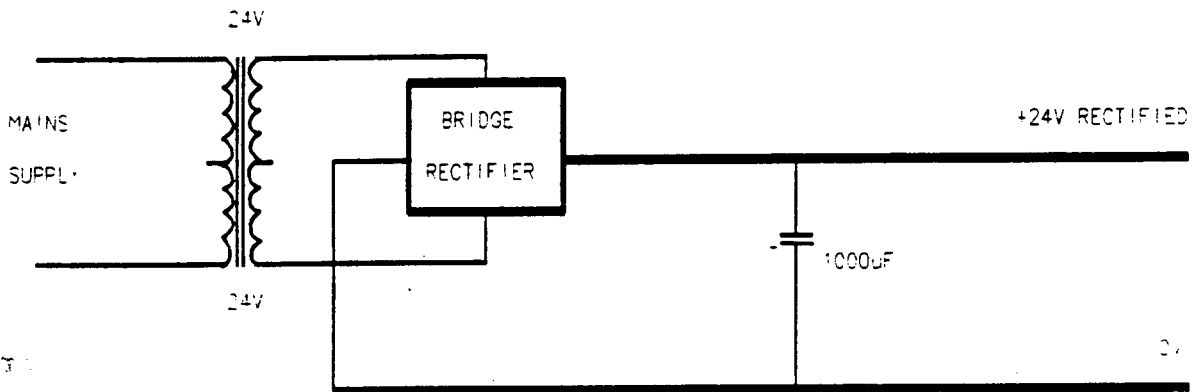
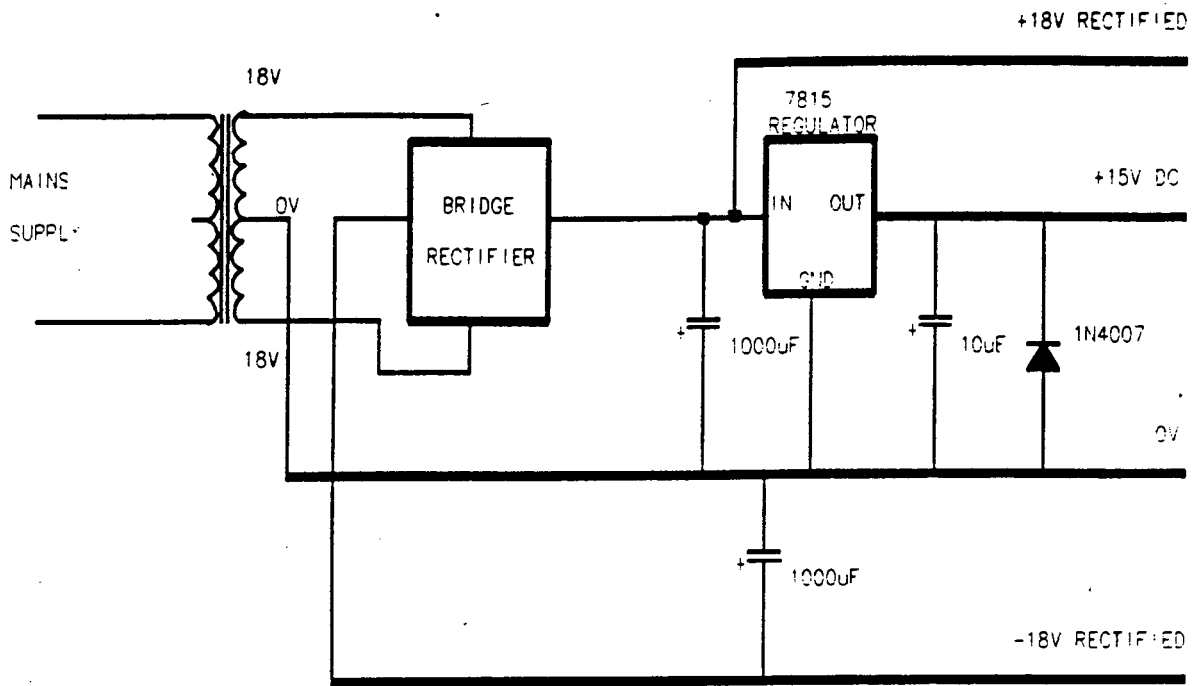


Figure 3-17 MAIN POWER SUPPLY CIRCUIT

The centre tapped secondary windings of the mains transformer are adequately rated at 18V-0V-18V and 24V-0V at 2 amps. The transformer output is rectified by means of bridge rectifiers. The outputs of the rectifiers are smoothed using 1000 microfarad electrolytic capacitors rated at 50 volts. The positive 18 volt

rail is regulated using a 7815 voltage regulator to provide a stable +15 V supply rail for the decision logic. The output of the regulator is further smoothed by means of a 10 microfarad tantalum capacitor. The diode provides a short circuit protection for the power supply.

CHAPTER FOUR

PERFORMANCE OF THE LOW COST SYSTEM

4.1 *The Receiver*

The 1kHz receiver as described in Section 3.2 provides direct demodulation of the radio frequency input signal. The 1kHz signal is detected by rectification at a non-linear element which is a detector diode or "low-level detector" in this case. This detector operates in the square law region of its non-linear characteristic. Its rectified output voltage is directly proportional to the signal input power (square of the input voltage). The detector output voltage is amplified and this voltage is applied to the input of the frequency decoder.

This type of receiver can be characterized by four main features: sensitivity, dynamic range, bandwidth and power handling. The sensitivity of a receiver is its ability to detect the weakest possible signal, which may be of the order of or even weaker than the noise in the system. "Tangential sensitivity" indicates the ability of the detector to detect a signal against a noise background and includes the noise properties of the detector. It is defined as the amount of signal power, below a one milliwatt reference level, required to produce an output pulse whose amplitude is sufficient to raise

the noise fluctuations by an amount equal to the average noise level [9]. Tangential sensitivity corresponds to a signal-to-noise ratio of about 2.5 and is thus approximately 4dB above the signal. At the frequency of interest the manufacturer specifies a typical value for the tangential sensitivity P_{ts} as -45dBm.

The dynamic range (DR) of the receiver is given as the difference between the minimum detectable signal (MDS) and the maximum input signal that can be accepted before compression (CP) or undesirable intermodulation effects take place. Thus

$$DR = P_{CP} \text{ dBm} - P_{MDS} \text{ dBm}$$

for the diode used in the Gunn oscillator/detector module, the following values were specified

$$P_{ts} = P_{MDS} = -45\text{dBm} \quad \text{and} \quad P_{CP} = +7\text{dBm}$$

thus giving a dynamic range of 52dB.

With the following procedure the performance of the detector diode, neglecting any contributions from the amplifier could be determined. A frequency generator was used to simulate the 1kHz transmitter. Connected to the end of the oscillator module known amounts of power could be fed to the detector by adjusting the rotary vane attenuator indicated in Figure 4-1. By plotting the diode output power P_{out} as a function of the input power P_{in} , the 1dB compression point occurs where the experimental curve deviates from the ideal line by 1dB (Figure 4-2).

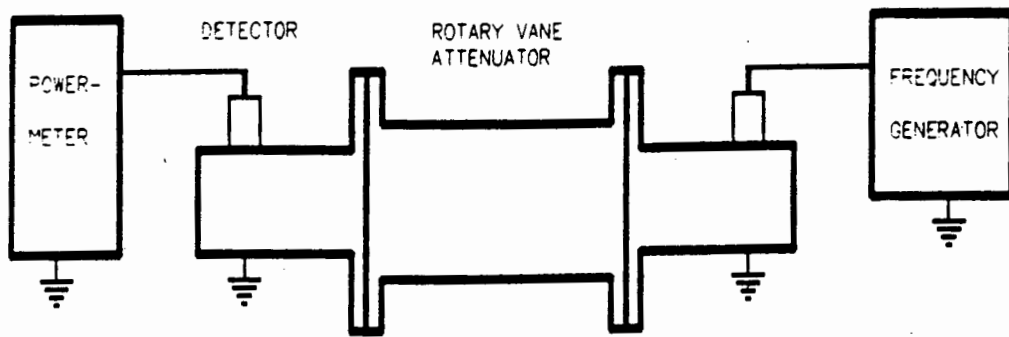


Figure 4-1 DETECTOR PERFORMANCE TEST SET UP

The two values are fixed in a direction perpendicular to the incident E-vector and the attenuation is varied by rotating the central section.

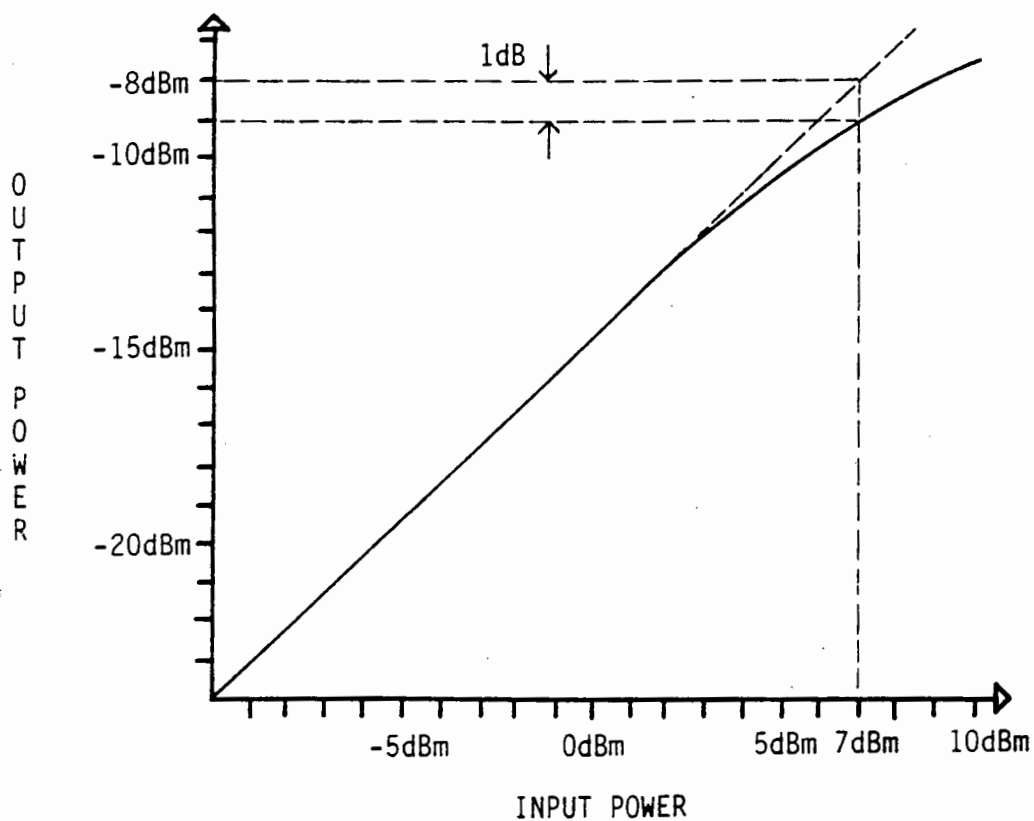


Figure 4-2 DYNAMIC RANGE COMPRESSION POINT

By taking the difference between the input power and the corresponding output power at the 1dB compression point, the conversion loss of the diode was determined to be 15dB. Figure 4-3 below shows a block diagram of the receiver. By adding the filter loss (8dB), the preamplifier gain (38dB) and the mixer conversion loss (15dB) an overall system gain of 15dB results.

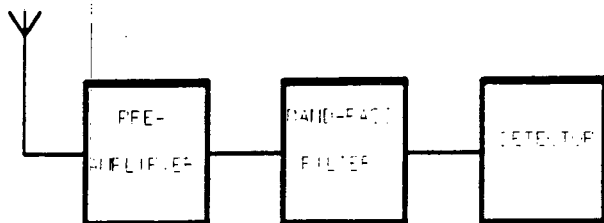


Figure 4-3 BLOCK DIAGRAM OF RECEIVER

4.2 Range Calculations

The power output of the Gunn oscillator module was measured to be 8.5mW using a power meter connected to the end of the waveguide cavity. In Section 3.5.1. the gain of the horn antennas used was calculated to be 15.6dB. The minimum detectable input power to the tone-decoder is specified as 20 mV at an input resistance of 20kohms. Thus the minimum detectable power P_{min} is

$$\begin{aligned}
 P_{min} &= (V^2/R) = (20 \times 10^{-3})^2 / (20 \times 10^3) &= 2 \times 10^{-8} \text{ W} \\
 & &= 2 \times 10^{-5} \text{ mW} \\
 & &= -47 \text{ dBm}
 \end{aligned}$$

At the input of the mixer the minimum detectable power is thus
 $-47\text{dBm} + 15\text{dB} = -32\text{dBm}$

Using all the above figures the maximum range of the unit can be evaluated by equating

$$R = \sqrt{\frac{P_{tx} G^2 \lambda^2}{P_{rx} (4\pi)^2}} = \sqrt{\frac{P_{tx}}{P_{rx}}} * \frac{G \lambda}{4\pi} = 11.2m$$

The values chosen in the calculation were either determined experimentally or where that was not possible the typical values as specified by the manufacturers were taken. Therefore the maximum achievable range as determined above should be in close accord with the experimentally determined range.

4.3 Range Measurements and Limitations

As described in chapter 3 the transmitter/receiver boards were built and supplied with a rectified voltage from a power supply via 50m of shielded cable. The message signals were run along the same shielded cable to the decision logic and relay configuration. An oscilloscope was used to monitor the detector diode output and the tone decoder output.

The two horns were aligned and moved apart along their common axis. The maximum operation range could then be determined by moving the horns until the low level alarm relay switched on, ie. once the tone decoder output went from low a to a high state. By closing the distance between the oscillators until the tone decoder moved back into lock the maximum operation

range of 9.8m was measured. With the transmitter and receiver 6.0m apart the expected signal strength at the receiver can be calculated using the expression below:

$$\begin{aligned} \text{signal strength} &= P_{TX} + 2 \times G + 20\log\lambda - 20\log R - 20\log(4\pi) \\ (\text{in dB}) & \\ &= 9.3\text{dBm} + 31.4\text{dB} - 30.7\text{dB} - 16.3\text{dB} - 22.0\text{dB} \\ &= -28.3\text{dBm} \end{aligned}$$

This value is just 1.7dB better than the minimum detectable power.

The insertion of pieces of microwave absorbent material into the signal path "extinguished" the beam beyond detection, i.e. the tone decoder went out of lock. However tests performed with 15cm thick concrete slabs in front of each horn antenna to simulate the shaft wall lining stressed the marginality of the system. Measurements with a Hewlett Packard network analyzer showed that at a frequency of 10.35GHz the microwave beam will experience an attenuation of around 5dB when passing through 30cm of concrete. Including this figure the signal strength at the receiver input reduces from -28.3dBm to -33.3dBm, which is less than the power necessary to trigger the tone decoder. This attenuation experienced by the microwave beam weakened it to such an extent that detection of the beam could not be guaranteed at all times with the transmitter and receiver 6m apart.

Variations in received signal level, or fading, in a microwave system cannot be predicted accurately. From observations made of the behaviour of existing microwave systems it has been determined that two types of fading are most prevalent. The first is caused by atmospheric conditions changing the reflection index of the medium and is termed beam bending. In the present application the transmission path is only 6m and thus fading due to beam bending can be ignored. The second type is called multipath fading and is the result of interference between two or more signals travelling over slightly different routes through the medium. This can be as much as 10dB or 15dB. As the length of the microwave path is increased, the number of possible indirect paths by which the signal may be received increases rapidly. The signals from these various indirect paths, when added to the direct signals, cause random field strength variations around the median signal value [10].

Considering a real situation where the level of kimberlite is not far below the signal path, the direct and various indirect signals reflecting off the kimberlite can cause total signal cancellation if the respective signals are equal in amplitude but opposed in phase.

4.4 Discussion

The performance of the low cost system proved to be more critical than expected. Due to multipath fading and general marginality of the system, false alarm messages are prone to be generated. One way of circumventing this detection problem is to increase the transmitter power. However the use of a 50mW transmitter only increases the signal to noise ratio by 7dB. But even this new improved signal strength can be considered borderline because of the effects of multipath. To compensate for this effect the transmit power needs to be increased to 43dBm (19 watts) in the worst case of a multipath loss of 15dB (obtained using the range equation). In addition the antennas have to be aligned to achieve a range in the proximity of the maximum value calculated.

Other microwave power generators that can operate at much higher power levels, such as klystrons and magnetrons, are much more expensive than the Gunn device and become even more unattractive in this particular design because of their large physical dimensions and bulky power supplies. Another way of improving the detection range is to make the receiver more sensitive to small signal levels. A superheterodyne receiver will have a far better sensitivity than the system described here at the expense of increased complexity. The design of such a system is the topic of discussion in the following chapters.

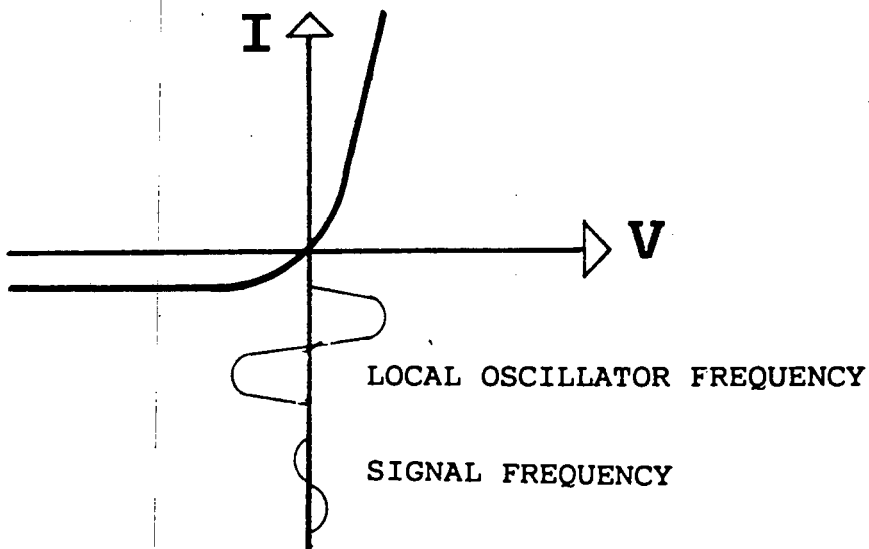
CHAPTER FIVE

DESIGN OF A SUPERHETERODYNE SYSTEM

5.1 The Superheterodyne Principle

A superheterodyne receiver is a receiver in which the incoming signal frequency is converted to a new lower value where most of the amplification takes place before detection. This is accomplished by means of a local oscillator (LO) and a non-linear rectifying element. The local oscillator and the signal are coupled into the non-linear device and generate among other frequencies the frequency difference between the signal and the local oscillator frequencies, normally termed the intermediate frequency (IF). Because the IF is fixed, the frequency response can be accurately determined using an appropriate filter. The local oscillator may be at a higher or lower frequency than the signal since only the difference is of interest. The IF amplitude is proportional to the signal amplitude and is substantially independent of the local oscillator voltage amplitude. The circuit containing the non-linear rectifying element is usually called "mixer" or "down-converter", and the process is referred to as mixing or frequency conversion. The non-linear device is usually a diode rectifier known as a "mixer diode". Application of the local

oscillator and signal voltages to a mixer diode is shown as the diode current-voltage characteristic in Figure 5-1 below.



Figure, 5-1 APPLICATION OF LOCAL OSCILLATOR AND SIGNAL VOLTAGES TO A MIXER DIODE

The local oscillator voltage is adjusted to a much higher level than that of the signal in order to bias the signal voltage to the optimum region of the mixer diode.

A block diagram of a simple superheterodyne receiver is shown in Figure 5-2. The mixer is followed by an IF amplifier since amplification at this stage is more easily provided than at the microwave frequency. This amplified signal is then filtered and applied to the input of the detection circuitry.

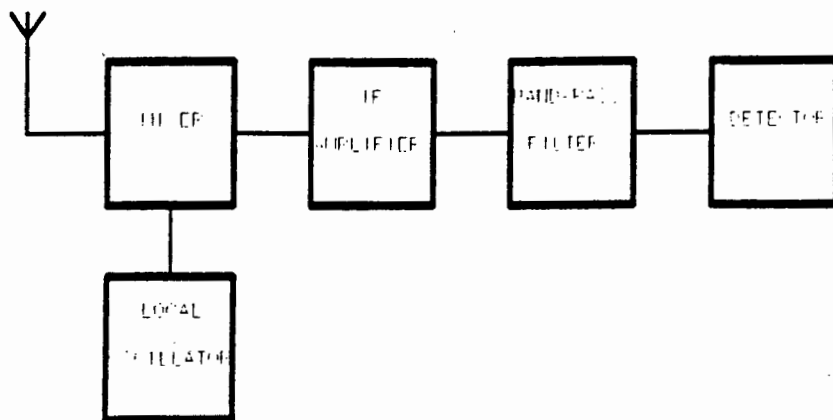


Figure 5-2 *BLOCK DIAGRAM OF A SIMPLE SUPERHETERODYNE RECEIVER*

5.2 *The Superheterodyne System Layout*

The output frequency of an oscillator generally varies considerably with temperature, which is very problematic in a superheterodyne receiver. To ensure that the mixer converts the input signal to the correct intermediate frequency, the local oscillator in the receiver has to remain in tune with the transmitter voltage controlled oscillator (VCO). This can be achieved by employing crystal oscillator circuits at both the transmit and receive end of the system. Frequency stability of a few parts per million over normal temperature ranges can be achieved in this manner. A more sophisticated technique involves electronic automatic frequency control in the receiver circuit of which many variations are possible. In this design

the transmit VCO is allowed to "float" at the microwave frequency while the frequency of the receive VCO is adjusted electronically to provide a constant intermediate frequency to the IF amplifier. Electronic tuning is facilitated by a varactor diode mounted inside the waveguide cavity next to the Gunn diode. Figure 5-3 shows the proposed system layout.

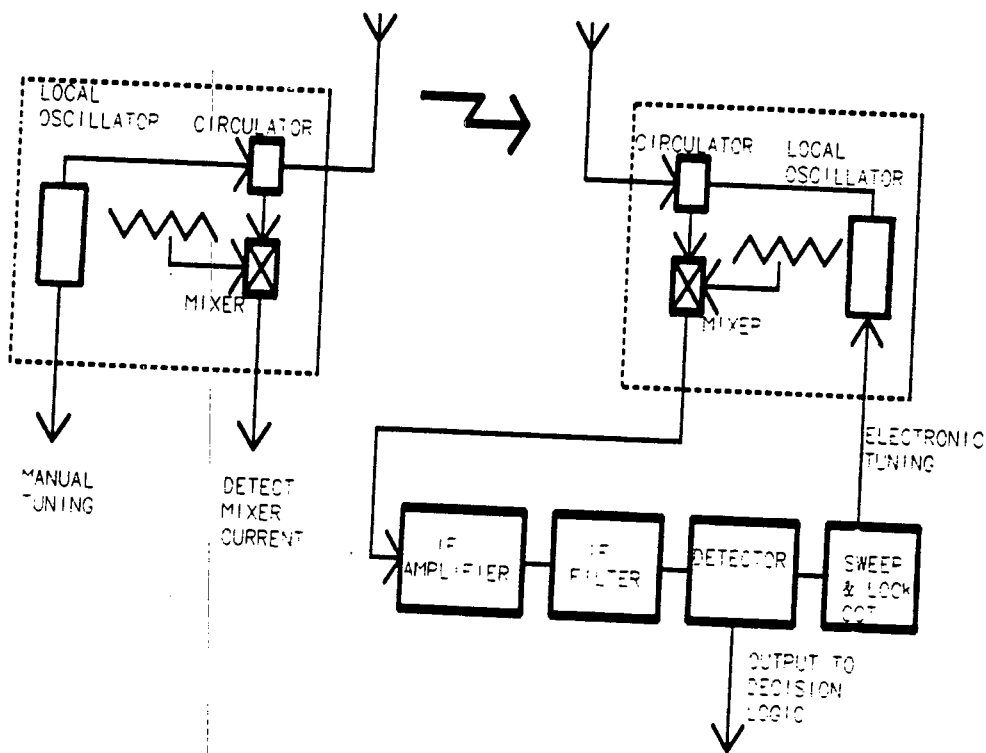


Figure 5-3 BLOCK DIAGRAM OF PROPOSED SYSTEM

The operating frequency of the system remains at 10.35GHz. In comparison with the low cost system the transmitter is simplified considerably as there is no need for pulsing the VCO output frequency.

The received microwave signal is mixed down to an intermediate frequency of 10.7MHz and is fed via an IF amplifier through the IF filter to a detector. The detector output is linked to the same decision logic circuit boards as described in subsection 3.6.1.

The output of the detector is also fed to a sweep-and-lock circuit which generates the correct bias voltage for the varactor, thereby keeping the local oscillator frequency in the receiver in tune with the transmitter VCO.

Section 3-1 deals with the self-checking mechanism of the low cost unit. The function check simplifies considerably in the superheterodyne system. In the transmitter VCO shown in Figure 5-3 some of the power generated "spills over" to the mixer diode, resulting in an output power of around 2.5mW with no signal present at the input port of the waveguide cavity. The mixer diode output current can thus be used to determine whether or not the VCO is transmitting any power. On the receiver end the same principle can be applied, in this case to verify the correct functioning of the mixer.

5.3 The Varactor Tuned Gunn Oscillator

This type of device uses the properties of a reverse biased diode to change the resonant frequency of a Gunn oscillator. As the reverse bias across the P-N junction of the varactor diode is increased, the depletion region between the two junctions widens and therefore increases the exposed charge. Accordingly a capacitance is formed between the non-conductive depletion layer and the junction. This capacitance varies with a change in reverse bias, resulting in the term varicap diode or varactor diode. A large capacitance ratio C_{max}/C_{min} results in large changes in resonant frequency. The varactor tuned Gunn oscillator chosen as the basis for the superheterodyne system is a MA-87127 supplied by Microwaves Associates, Inc. A diagram of this device is shown in Figure 5-4 below.

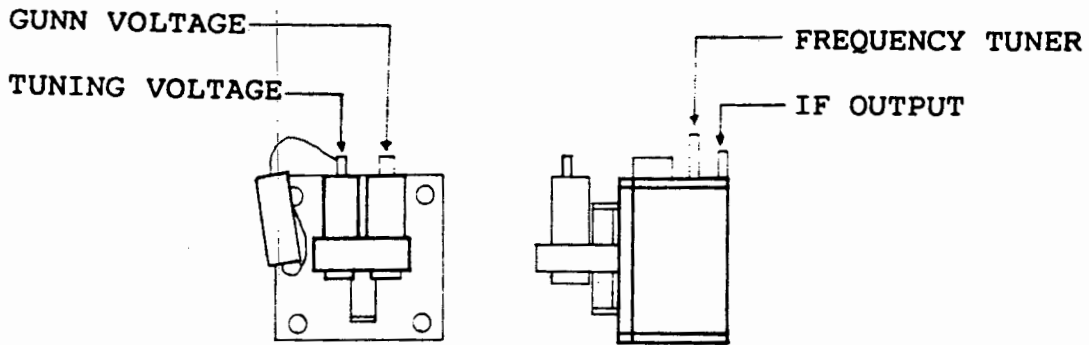


Figure 5-4 *OUTLINE DRAWING OF THE VARACTOR TUNED GUNN OSCILLATOR*

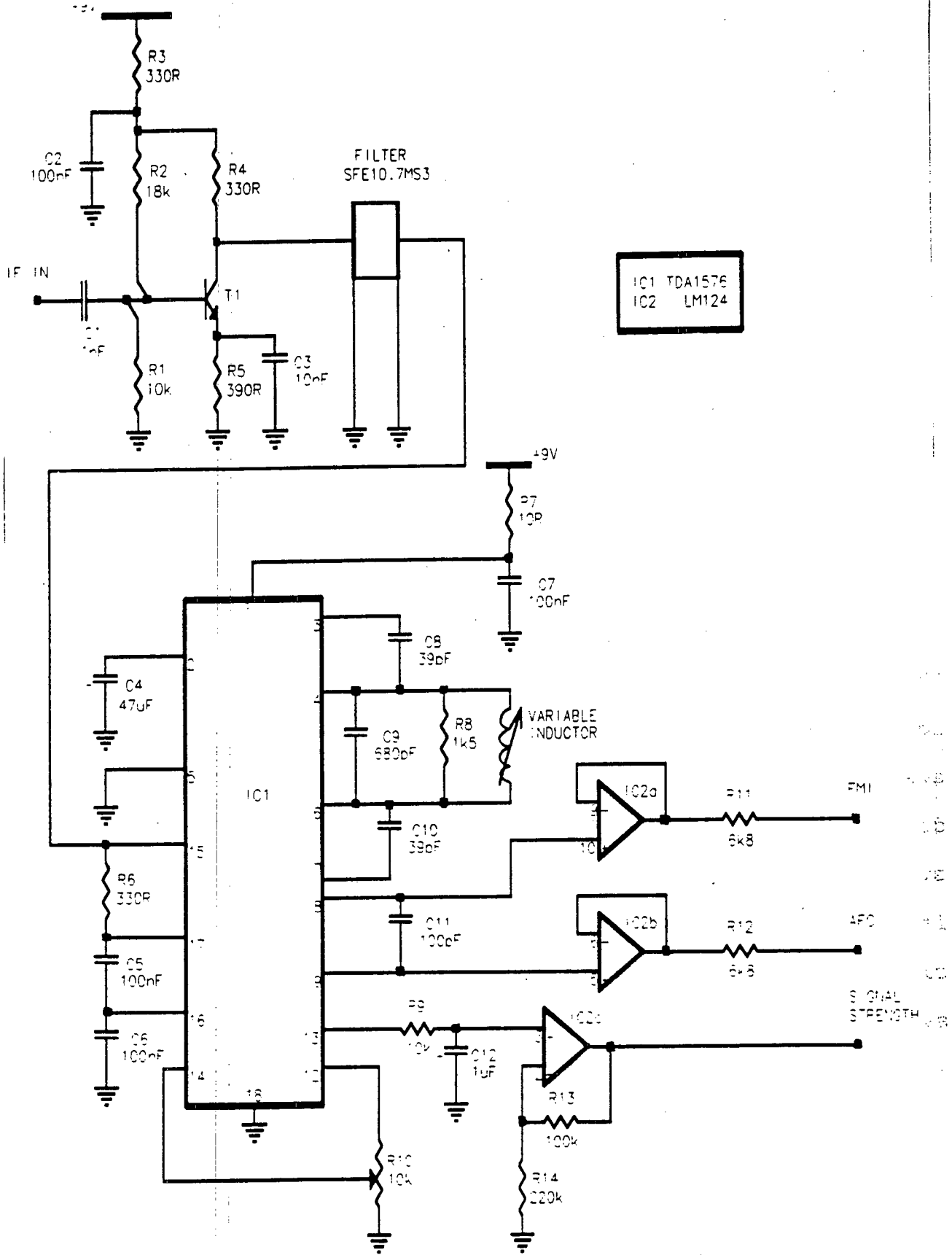
The oscillator has a centre frequency of 10.35GHz which can be shifted by $\pm 100\text{MHz}$ using mechanical tuning. The tuning varactor is mounted close to the Gunn diode and will deviate the

fundamental frequency by about 60MHz when the proper tuning voltage is applied. The Gunn diode acts simultaneously as a transmitter and a local oscillator with a portion of its energy (about 0.5mW) being coupled to the mixer diode. A ferrite circulator has been integrated into the waveguide mount to isolate the transmitter and receiver functions.

5.4 IF Amplifier and Detector Circuit Design

A circuit diagram of the IF amplifier is given in Figure 5-5. The 10.7MHz signal from the mixer is AC coupled via C_1 to a single stage common emitter amplifier T_1 . The amplifier provides a power gain of 200 (23dB) and the noise figure was 35dB. The amplified signal is fed through the ceramic filter F_1 which causes an insertion loss of 7dB. The filter results in a signal with a bandwidth of 250kHz with signals outside this bandwidth attenuated by 70dB. R_1 matches the impedance of the filter.

The signal is fed from the filter to IC_1 . IC_1 is a monolithic integrated FM/IF amplifier. It generates a symmetrical automatic frequency control (AFC) output in the form of a S-curve. The S-curve appears at pin 9 (AFC line) and its inverse at pin 8 (FMI line). The FM discriminator circuit is tuned externally by inductor L_1 and capacitor C_9 . R_8 de-Q's the resonant circuit to produce a more linear S-curve.



IC1 TDA1576
IC2 LM124

Figure 5-5 CIRCUIT DIAGRAM OF IF AMPLIFIER AND DETECTOR

Coupling is provided by C_8 and C_{10} . As the impedance of IC_1 is 3kohms, IC_{2a} and IC_{2b} provide buffering to prevent the sweep-and-lock circuit board from loading IC_1 . The AFC voltage is fed to the sweep-and-lock circuit board which ensures that the instruments stay in tune. The internal +5V reference is taken from pin 12 and is fed back to pin 14 via a potentiometer R_{10} to set the minimum signal strength voltage. The signal strength voltage is fed from pin 13 of IC_1 to a DC amplifier IC_{2c} and from there to the autotune circuit.

5.5 The Sweep-And-Lock Circuit Design

The sweep-and-lock circuit generates a ramp voltage which, when fed to the varactor, causes the local oscillator frequency to sweep across the transmitter frequency. When the IF circuit detects an S-curve the sweep-and-lock generates a pause command stops the ramp voltage and applies AFC. A full circuit diagram is provided in Figure 5-6. Because of the complexity of the circuit, its description is broken up into 3 parts; the sweep system, the sweep window detector and the pause control.

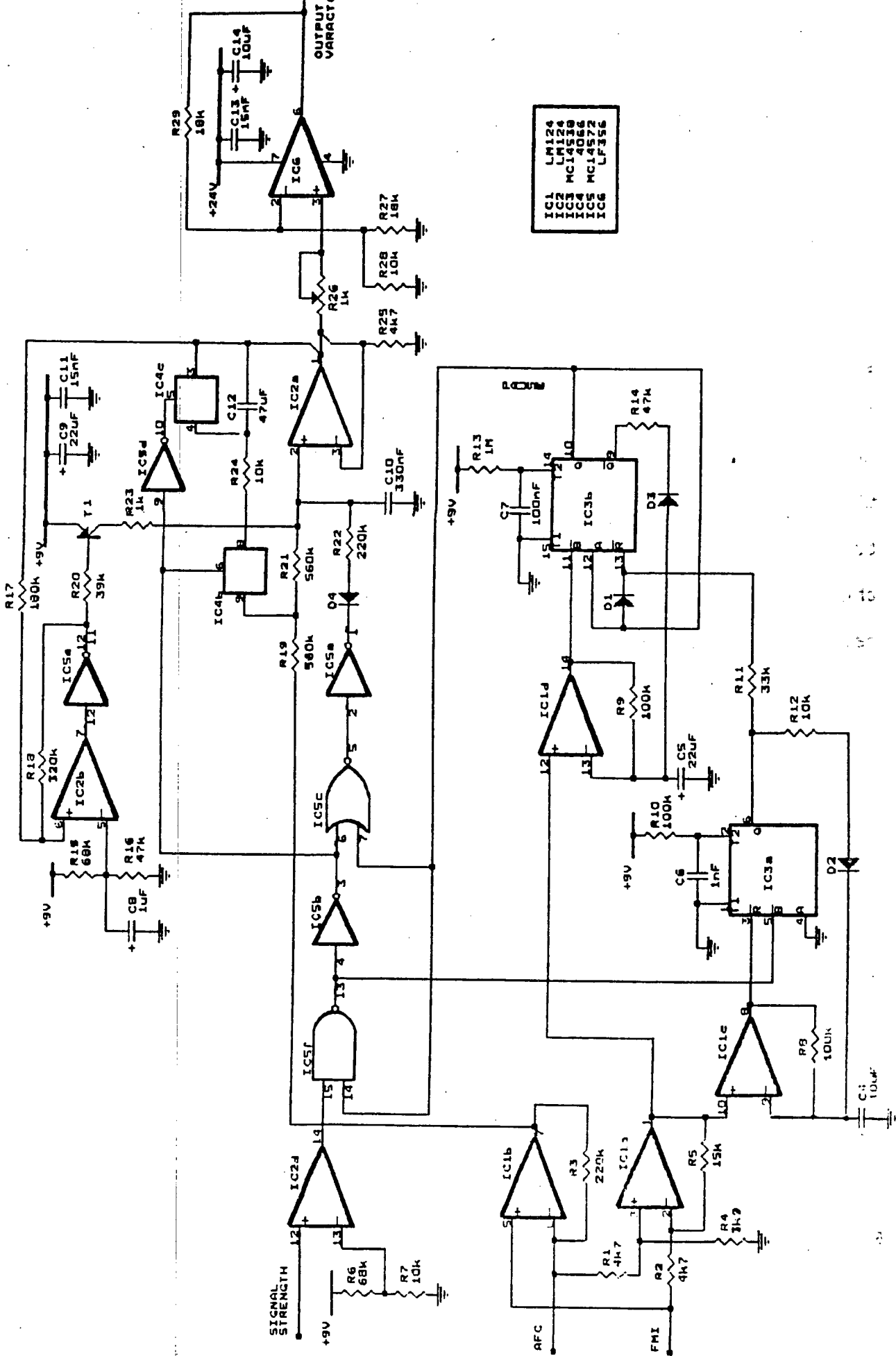


Figure 5-6 CIRCUIT DIAGRAM OF THE SWEEP-AND-LOCK

5.5.1 The Sweep System

Figure 5-7 shows the section of the sweep-and-lock circuit that is considered here. Until the signal is detected the output of IC_{2d} is low. With both inputs to NAND-gate IC_{5f} being low, its output at pin 13 will be high. IC_{5b} inverts this voltage and feeds it to pin 6 of the NOR-gate IC_{5c} which controls the sweep. If the input from the pause control IC_{3b} is also at logic 0, the output of IC_{5c} will be at logic 1. By inverting this signal via IC_{5a}, diode D₄ is forward biased. This is the condition for sweeping. The logic 0 at IC_{5b} is also fed to switch off IC_{4a} thereby removing the effect of R₂₄. At the "same" time IC_{4d} is switched on (via inverter IC_{5d}) and capacitor C₁₂ is allowed to discharge.

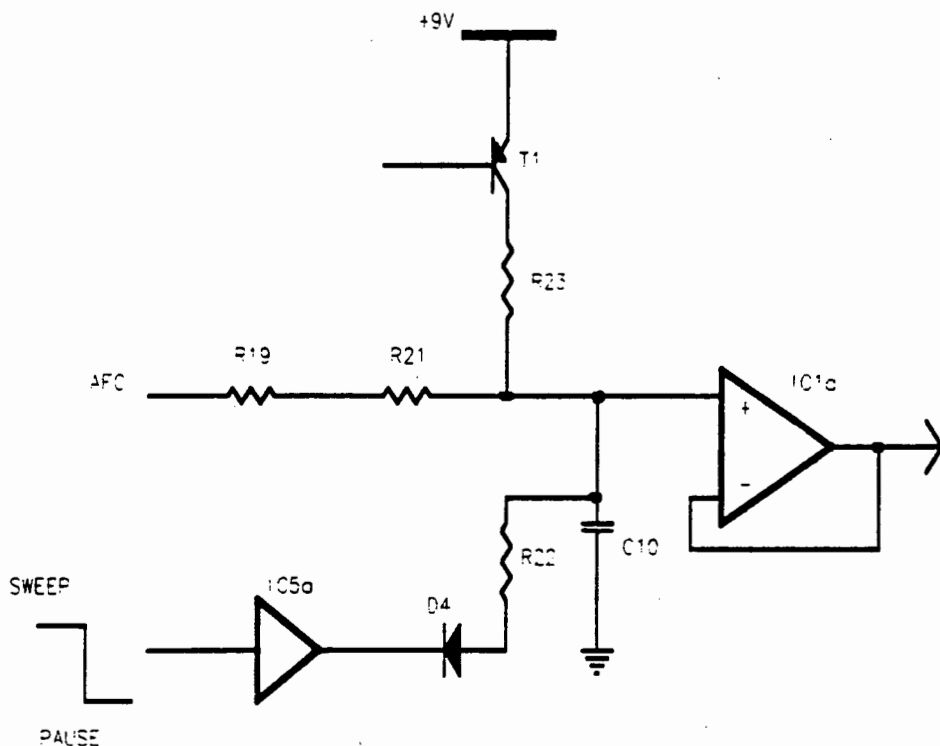


Figure 5-7 SWEEP SYSTEM CIRCUIT DIAGRAM

With IC_{5a} output at logic 0, the sawtooth type sweep or search voltage is generated by C_{10} rapidly charging to a predetermined upper voltage level by means of transistor T_1 via R_{23} . When T_1 is switched off, C_{10} can discharge through R_{22} . This resistor is smaller in value than the series connection of R_{19} and R_{21} and thus largely controls the discharge rate of C_{10} . Once the predetermined lower voltage limit is reached, C_{10} is again rapidly charged to the upper voltage limit to re-initiate the cycle. This sawtooth waveform is buffered by IC_{2a} and fed via the level shifter IC_6 to the varactor diode on the Gunn oscillator module, thereby allowing the local oscillator frequency to sweep the allocated frequency band. The modulation index is set with R_{26} . To allow for a setting of the correct varactor voltage, the gain of IC_6 is adjustable by select-on-test (SOT) resistors where R_{27} is the coarse setting and R_{28} for fine adjustment.

If the pause control goes high during the discharge portion of the sweep cycle, the voltage across C_{10} will be momentarily frozen since the now reverse biased diode D_4 effectively disconnects R_{22} . The output of the circuit and hence the varactor voltage will be held constant.

This in turn will keep the local oscillator voltage constant. If the local oscillator and the received carrier frequency

differ by an amount equal to the intermediate frequency of 10.7MHz, the IF amplifier will amplify this difference. The signal strength output will be compared to a set value determined by the potential divider R_6 and R_7 . If the signal strength is larger the output of IC_{2d} will go high. Switch IC_{4a} is switched on and R_{24} and C_{12} are connected across IC_{2a} . At the same time NAND-gate IC_{5f} has now two high inputs and is thus forced to output a logic 0. This is inverted by IC_{5b} and fed to NOR-gate IC_{5c} , forcing its output to a logic 0 and thereby removing the effect of R_{22} since diode D_4 is again reverse biased.

As a result of these actions, IC_{2a} is converted into an AFC filter, essentially of a Sallen and Key type with the exception of R_{24} (see Figure 5-8). This is added to give a transmission zero in order to achieve AFC loop stability.

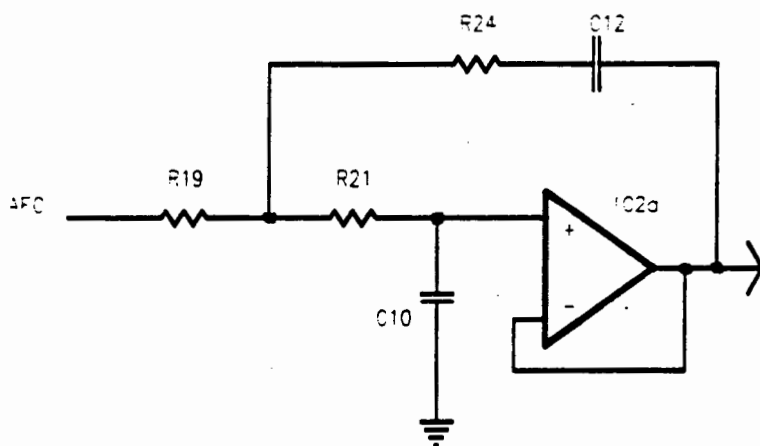


Figure 5-8 SALLEN AND KEY TYPE FILTER

The input to IC_{2a} is taken from the differential amplifier IC_{2b} . IC_{2b} has a very high gain and acts as a comparator, continuously comparing the voltage levels of the AFC and FMI signals from the frequency discriminator. If the local oscillator frequency increases, the IF difference frequency increases and the voltage on the AFC line increases while that on the FMI decreases. This results in a falling composite waveform at the output of IC_{1b} . This waveform is then filtered by the filter shown in Figure 40. The lowered output of IC_{2a} reduces the varactor voltage and consequently the local oscillator frequency. Conversely a decrease in the LO frequency will result in an increased output at IC_{2a} . In this way automatic frequency control is achieved. If however the received signal is not recognized, i.e. the signal strength output is too low, R_{22} will again be applied after the short pause time set by the pause control.

5.5.2 The Sweep Window Detector

The functioning of the sweep window detector is best explained by focusing on the part of the sweep-and-lock circuit that is copied in Figure 5-9 on the following page.

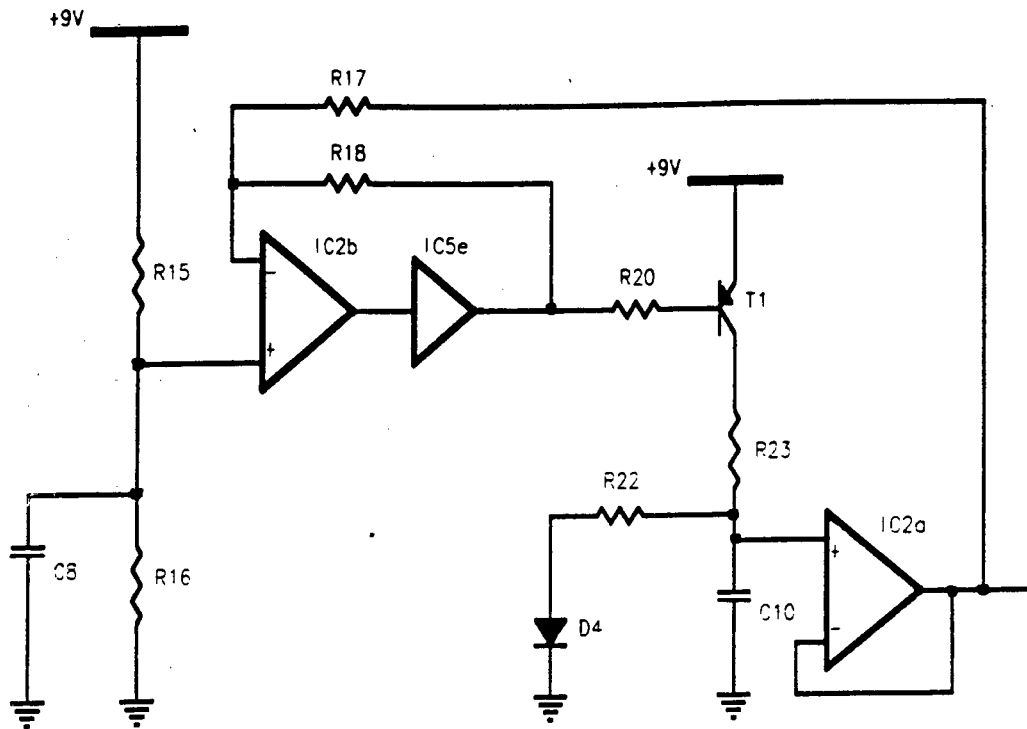


Figure 5-9 SWEEP WINDOW DETECTOR CIRCUIT

Operational amplifier IC_{2b} acts as a comparator with IC_{5e} ensuring that the high and low output voltages are well defined. The voltage inversion caused by IC_{5e} effectively transposes the polarity of the input terminals on IC_{2b}. The reference voltage developed by dividers R₁₅ and R₁₆ and the well regulated 9 volts supply gives a well defined voltage level of 4 volts. The limits of the sweep are thus accurately set.

In the discharge region of the sweep cycle the transistor T₁ is switched off and the output of IC_{5e} is high and within a few millivolts of the 9 volt supply. Resistors R₁₇ and R₁₈ set the bandwidth of the sweep. At some stage the output

voltage of IC_{2a} becomes so low that comparator IC_{2b} changes state, i.e. its output goes high and the IC_{5e} output falls. This output is fed back to the inverting input of the comparator via R_{18} , thereby pulling the input voltage even further down and achieving positive feedback.

Transistor T_1 is thus switched on and allows C_{10} to charge up via R_{23} . The voltage divider formed by R_{17} and R_{18} now compares the output of IC_{2a} to the 4 volt reference voltage. When this is exceeded, the comparator changes state again and positive feedback pulls R_{20} up to the supply. The transistor is switched off and C_{10} can discharge via R_{22} . Diode D_4 allows a repeat of the sweep cycle.

5.5.3 The Pause Control

In the initial stages of the tuning process the local oscillator searches for the received signal by sweeping in the frequency band around it. The search is made to pause when a carrier in the allocated frequency band is detected. This is achieved by the pause control which consists of IC_{1a} , IC_{1c} , IC_{1d} , IC_{3a} and IC_{3b} . IC_{1a} amplified the difference between the AFC and FMI outputs of the IF detector circuit and since IC_{1a} is a differential amplifier all common mode noise is effectively removed.

Now consider Figure 5-10 below. The output of IC_{1a} is fed to IC_{1d}. With zero voltage across capacitor C₅, diode D₃ is reverse biased and C₅ commences to charge via R₉ until it exceeds the negative spike level of the non-inverting input. The output of comparator IC_{1d} goes to zero and C₅ is discharged through D₃ and R₁₄, until the input voltage again exceeds the capacitor voltage. The width of pulses generated at the output of IC_{1d} are related to the amplitude and duration of the negative peaks of the input signal. The ratio of the "on" to "off" times of the output is only dependant on the ratio of resistors R₉ and R₁₄ and the average DC value of the input. It can thus be said that the comparator output "rides" on the negative peaks of the input signal. Similarly comparator IC_{1c} "rides" on the positive first peaks of the input signal.

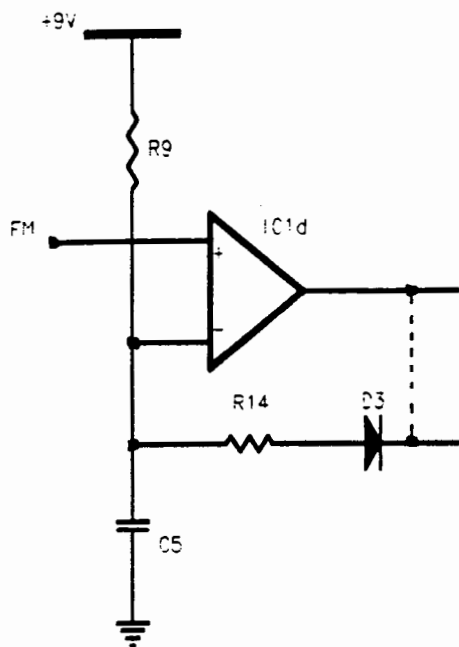


Figure 5-10 SECTION OF THE PAUSE CONTROL CIRCUIT

In Figure 5-6 diodes D_2 and D_3 are connected to the outputs of the multi-vibrators IC_{3a} and IC_{3b} respectively. The output "on" time becomes fixed in each case and the average mark/space ratios of the outputs are now determined by resistors R_9 and R_{14} (IC_{3b}) and R_9 and R_{12} (IC_{3a}). C_5 is allowed to charge to +9V via R_9 and would remain charged were R_9 not connected to the output of IC_{1d} . C_5 will again discharge when the output of IC_{1d} goes low. By connecting the Q output of IC_{3a} to the reset control of IC_{3b} , "windows" are created whereby IC_{3a} can only be triggered during an "on" time of IC_{3a} . Therefore, a normal "FM characteristic", where the signal initially goes positive (output from IC_{3a}) and then negative (giving an output from IC_{3b}) through the reset signals being removed, results in a fixed length output pulse. This pulse is the pause control and is about 100ms long. The positive-going pause pulse forces the output of NOR-gate IC_{5c} to go low. IC_{5a} inverts this output and reverse biases diode D_4 thereby removing the discharge path for C_{10} . The voltage of C_{10} is thus frozen resulting in the local oscillator frequency stopping in its sweep. If the signal strength output is high enough, lock will be achieved. The falling output of IC_{5f} resets the multivibrator IC_{3b} . In this manner the pause control is disabled when lock is achieved and thus reduces interference.

CHAPTER SIX

PERFORMANCE OF THE SUPERHETERODYNE SYSTEM

6.1 Mixer Diode Conversion Loss Measurements

The mixer or frequency conversion stage in the block diagram of Figure 5-3 assumes an important place in the superheterodyne receiver. Mixing may be broadly defined as the conversion of a signal from one frequency to another by combining it with the local oscillator frequency in the mixer diode. The mixing process however results in a complex frequency spectrum. The frequencies of major interest are shown in Figure 6-1 and consisting of the local oscillator (LO), the local oscillator harmonics (nLO), the intermediate (IF), the signal ($LO + IF$), the image ($LO - IF$) and harmonic sidebands ($nLO \pm IF$).

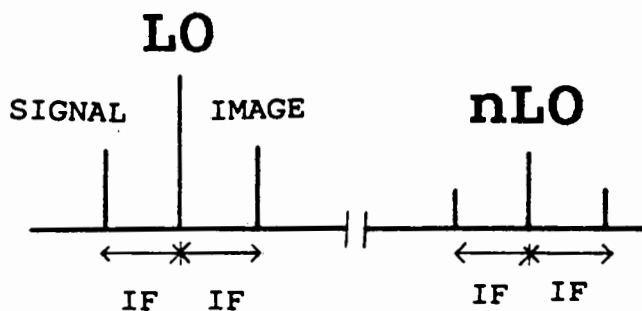


Figure 6-1 MIXER SPECTRAL DIAGRAM

The image frequency is of special importance on two counts. It is generated as a result of the direct beat between the signal

and the local oscillator second harmonic and also as a result of the beat between the IF and LO. The power consumed is taken from the available signal power, resulting in a lower conversion efficiency. The theoretical limit for the diode conversion loss is thus 3dB which is half the signal power that is converted to image power. The conversion loss L of a mixer diode may be represented by

$$L = \frac{P_S}{P_{IF}} = \frac{\text{signal power available at the input terminal}}{\text{IF power available at the output terminal}}$$

The conversion loss of the mixer diode was measured using the test set-up in Figure 6-2 below.

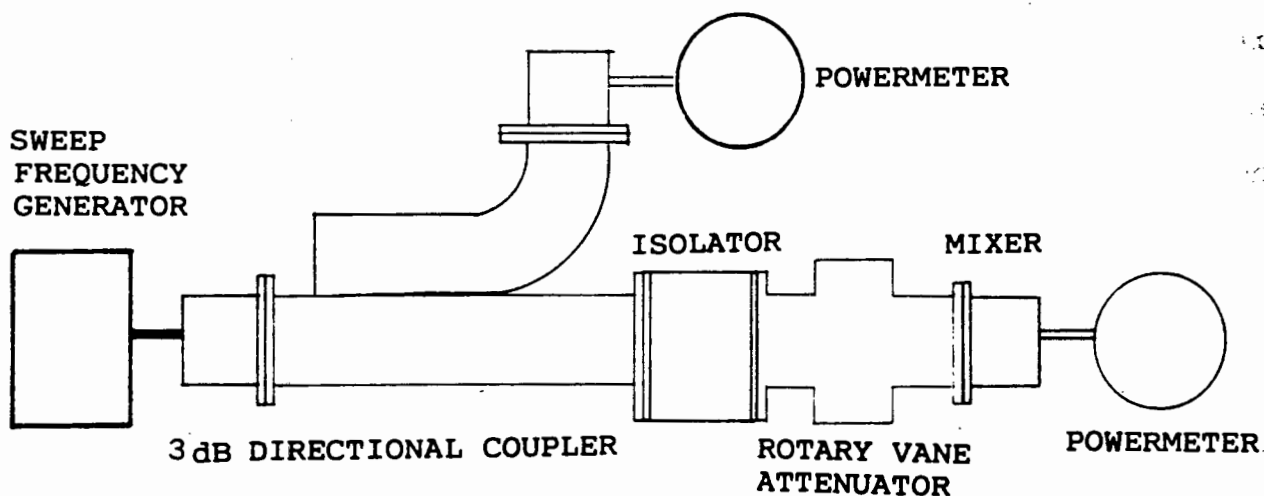


Figure 6-2 TEST SET-UP FOR CONVERSION LOSS MEASUREMENT

A sweep generator set to a frequency of 10.210GHz was used as a power source. A 3dB directional coupler in conjunction with a rotary vane attenuator was connected between the sweep and the mixer. In this way a known amount of power could be fed into the mixer. A ferrite isolator provided isolation between the source and the mixer. With the sweep set at 10ms and an output of 1mW, 5uW was fed into the mixer. By varying the frequency of the sweep generator the IF power output was measured for IF frequencies ranging from 1MHz to 400MHz. Table 1 shows the experimentally determined results and the respective conversion losses.

It can be seen from the above figures that at an intermediate frequency of around 10MHz the conversion loss is close to optimum. The increase in conversion loss above 250MHz is due to the high output capacitance of the mixer choke. Keeping the IF frequency fixed at 10.7MHz the conversion loss figures could be determined for varying input powers. Experimental results are shown in Table 2.

IF (in MHz)	IF power (in uW)	Conversion loss L (in dB)
1	0.64	8.9
2	0.69	8.6
5	0.69	8.6
10	0.69	8.6
20	0.69	8.6
30	0.70	8.5
40	0.70	8.5
50	0.72	8.4
60	0.74	8.3
70	0.78	8.1
80	0.80	8.0
90	0.82	7.9
100	0.83	7.8
150	0.86	7.7
200	0.75	8.2
250	0.53	9.8
300	0.32	11.9
350	0.19	14.2
400	0.10	16.9

Table 1 MIXER DIODE CONVERSION LOSS FIXED INPUT POWER

I/P Power (in dBm)	O/P Power (in dBm)	Conversion loss (in dB)
-35.5	-41.3	5.8
-32.2	-38.3	6.1
-31.0	-37.6	6.6
-29.2	-36.5	7.3
-27.7	-35.4	7.7
-27.0	-34.8	7.8
-24.6	-33.0	8.4
-23.0	-31.5	8.5
-20.0	-28.6	8.6
-14.6	-23.4	8.8
-12.6	-21.5	8.9
-10.5	-19.4	8.9
-9.7	-18.4	8.7
-7.7	-16.4	8.7
-5.8	-14.5	8.7
-2.7	-11.5	8.8
-0.7	-9.7	9.0
1.3	-8.0	9.3
3.3	-6.8	10.1
5.3	-6.1	11.4
7.2	-5.8	13.3
9.2	-5.5	14.7

Table 2 MIXER DIODE CONVERSION LOSS FOR FIXED IF

These values are plotted in Figure 6-3. The 1dB compression point was found at an input power of 5.2dBm (3.31mW).

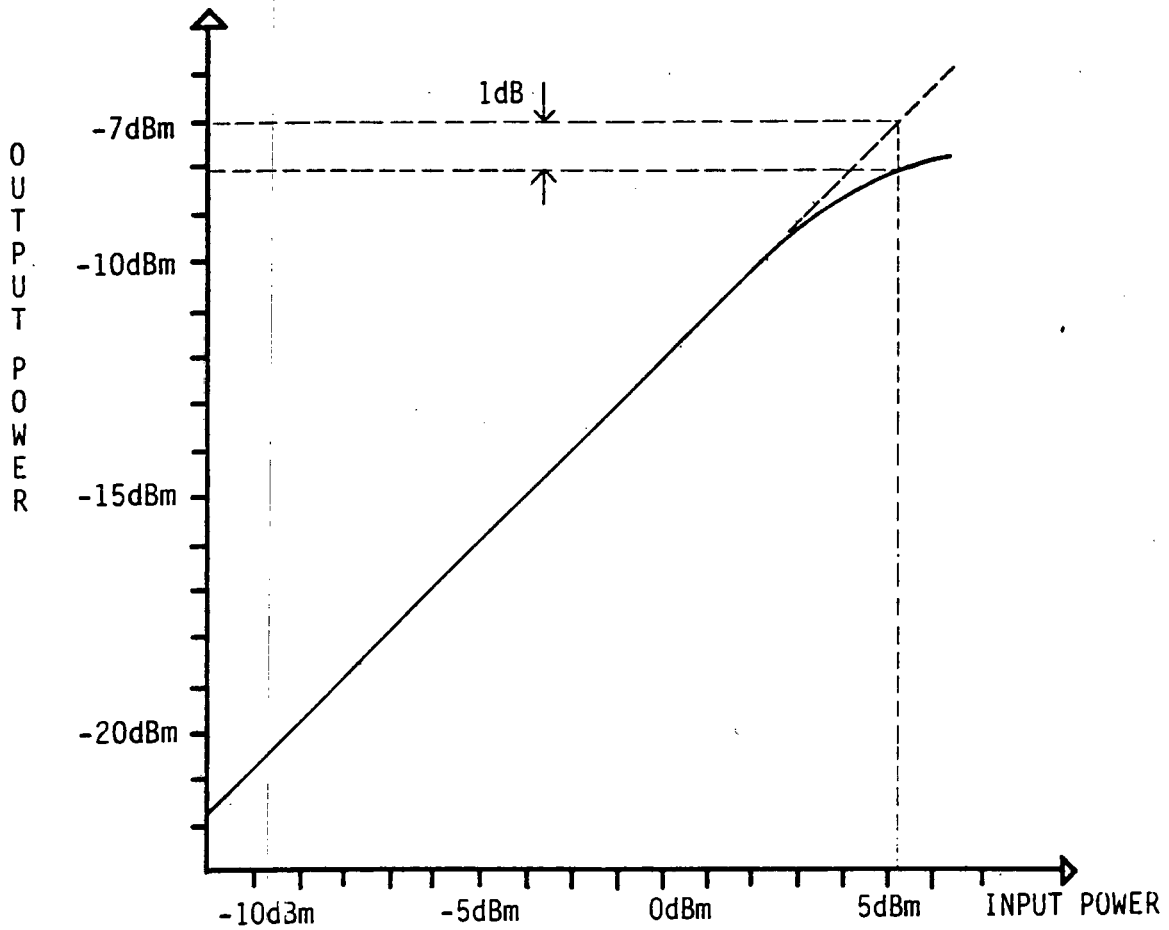


Figure 6-3 MIXER DIODE 1DB COMPRESSION POINT

6.2 Receiver Sensitivity Calculations

The minimum detectable signal in a receiver is determined by the noise power P_N at the input of the receiver.

$$P_N = kTB \quad \text{where } k = \text{Boltzman's constant}$$

T = temperature in ° K

B = bandwidth in Hz

The bandwidth used in the equation above is given by the IF filter bandwidth and is equal to 220kHz for the filter used.

Thus the noise power at the input is

$$\begin{aligned} P_N &= (1.38 \times 10^{-23}) (295) (220 \times 10^3) \\ &= 1.01 \times 10^{-15} \text{ watts} \\ &= -119.9 \text{ dBm} \end{aligned}$$

Due to the image frequency an additional 3dB noise power is thus present in a superheterodyne receiver, resulting in an effective noise power of -116.9dBm at the input to the receiver. However the mixer and amplifier stages degrade the signal to noise ratio even more. The noise figure is a measure of this degradation. It is defined as the difference in dB of input signal to noise ratio (SNR) and output SNR. Consider the block diagram of the receiver in Figure 6-4. The overall receiver noise factor NF is determined by the expression

$$NF = F_1 + \frac{F_2 - 1}{G_1} + \frac{F_3 - 1}{G_1 G_2}$$

where F_1 = mixer noise factor
 F_2 = IF amp noise factor
 F_3 = filter noise factor
 G_1 = mixer gain
 G_2 = IF amp gain

The mixer diode noise figure is equal to the conversion loss plus added noise. The added noise in a mixer diode is predominantly the noise generated by the parasitic resistance of the active layer. Other added noise sources are shot noise (due to electron flow across junction) and noise due to trapping of electrons in the junction (1/f noise). Typically the added noise amounts to 0.5dB, bringing the total mixer noise figure at an IF of 10.7MHz to 9.1dB ($F_1 = 8.12$). The noise figure of the IF amplifier was measured to be 3.5dB ($F_2 = 2.24$) and the IF amplifier gain equals 12dB ($G_2 = 16.8$). The mixer conversion loss was determined earlier as -8.6dB ($G_1 = 0.138$). Thus for a filter conversion loss of 2dB ($F_3 = 1.68$), the noise factor F equals

$$F = 8.12 + \frac{2.24 - 1}{0.138} + \frac{1.68 - 1}{0.138 \times 16.8}$$

$$= 17.40 \text{ (12.9dB)}$$

The noise level at the input to the receiver is increased by this factor. Thus the equivalent noise power at the input

$$P_N = -116.8\text{dBm} + 12.4\text{dB} = -104.5\text{dBm}$$

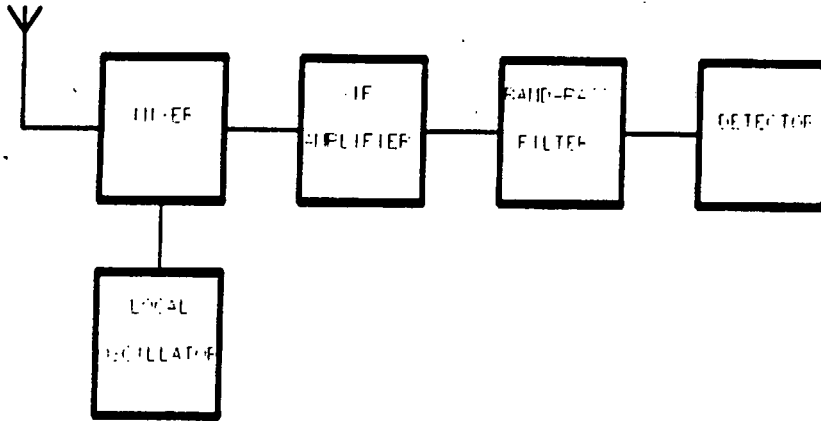


Figure 6-4 RECEIVER BLOCK DIAGRAM

The minimum voltage level that triggered off the frequency discriminator when applied to the input of the IF amplifier was 60uV peak to peak. The IF amplifier had an input impedance of 125ohms. Thus the minimum detectable signal (MDS) at the input to the IF amplifier was

$$\begin{aligned}
 P_{IF} &= \frac{(V_{RMS})^2}{R} = \frac{(60/2/2)^2}{125} \\
 &= 3.63 \times 10^{-9} \text{mW} \\
 &= -84.4\text{dBm}
 \end{aligned}$$

The range R over which the superheterodyne system needs to operate is 6.5m (including the concrete lining of the shaft walls). Thus the expected signal strength at the receiver can be calculated using the expression below:

$$\begin{aligned}\text{Signal strength} &= P_{Tx} + 2 \times G + 20\log\lambda - 20\log R - 20\log(4\pi) \\ (\text{in dB}) & \\ &= 19.3\text{dBm} + 31.4\text{dB} - 30.7\text{dB} - 16.0\text{dB} - 22.0\text{dB} \\ &= -18.0\text{dBm}\end{aligned}$$

As discussed above, the minimum detectable signal is a function of the noise at the receiver input. However if too much signal power enters the receiver, the mixer diode starts to saturate, thereby setting a limit for the maximum signal strength with which the unit will operate. The power absorbed by the mixer is a contribution of the input signal and of the local oscillator. As shown in Figure 6-3 the 1dB compression point was found at a signal power of 2.34mW. To measure the power coupled from the local oscillator into the mixer, the test set-up shown in Figure 6-5 was used.

The voltage drop across the 1ohm resistor mounted in parallel with the mixer diode was measured with the local oscillator on and no signal present. Then, with the LO off, a signal generator was used to drive the mixer until the voltage drop across the resistor equalled the previously determined value.

Since the voltage drops are the same, the power supplied by the signal generator (2.14mW) is a measure of the local oscillator power. The power required to saturate the mixer is thus the sum of the signal (3.31mW) and the local oscillator power (2.14mW) and amounts to 5.45mW (+ 7.4dBm).

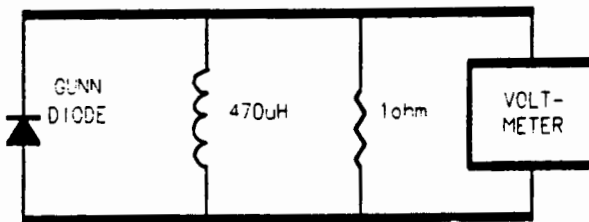


Figure 6-5 DETERMINATION OF LOCAL OSCILLATOR POWER

CHAPTER SEVEN

CONCLUSIONS

In Chapter 1 the system requirements for the ore level detector were laid out. A transmitter/receiver unit had to be designed to indicate when the ore level in a vertical ore chute falls below the level of the signal path between the transmitter and the receiver. The system also needs to indicate when either the transmitter, the receiver or both experience a malfunction. The two most common methods of detecting a microwave signal were discussed in Chapter 2. They are based on the low level detector and the superheterodyne principle. At this stage of the project the sensitivity of the receiver was of minor importance and thus a receiver based on the low level detection principle was preferred because of its simplicity. The commercial availability of a Gunn oscillator with an integral detector module helped considerably in the design of the system. Chapter 3 describes the design and construction of this low cost system.

However, tests performed with the unit stressed the marginality of its operating range. At a transmit power level of 9.3dBm, the available signal strength at the receiver situated 6m from the transmitter was measured to be -28.3dBm and the minimum detectable signal by the receiver is -30dBm, which only allows for a 1.7dB fade margin. The insertion of 30cm thick concrete

slabs degraded the signal by a further 5dB, thereby making it impossible to guarantee detection. The effects of multipath fading add an estimated 15dB of degradation, and thus decreasing the received signal strength even further to a value of -48.3dBm. At this point the decision had to be made to either increase the transmit power of the oscillator or to increase the sensitivity of the receiver. As the transmit power has to be increased by at least 20dB in order to just cover the effects of the degradation, the second alternative was preferred.

In Chapter 5 the design of the more sensitive superheterodyne receiver was considered. The transmitter used in this system has an output power of 19.3dBm, and is thus ten times higher than the transmit power level in the low cost system. Consequently, the signal strength at the receiver (at a distance of .6m from the transmitter) was -18dBm which is 10dB better because of the more powerful transmitter. Tests showed that the sensitivity of the superheterodyne receiver is -75.8dBm, an improvement of over 45dB in comparison with the low level detector. This increase in sensitivity can cope easily with the degradation due to the concrete and the multipath fading, with still a large amount of signal power to spare. In addition the superheterodyne system exhibited an improved dynamic range performance (81.0dB as compared to 52.0dB). In order for the low cost system to compete with the superheterodyne system, its

transmitter output power has to be increased by 45.8dB the increase in sensitivity) to 55dBm (316 watts). However such high power level can only be achieved using valve-type devices. However, because of the high cost and the complexity of the required power supplies for such devices, they do not present an alternative to the highly sensitive superheterodyne system.

List of References

- [1] BIRD, D.: *"Finsch Mine"*, Mining Magazine, February 1987, pp 120-125

- [2] READ, W.T.: *"A Proposed Negative Resistance Diode"*, Bell System Technical Journal, Vol 37, pp 401-448, 1958

- [3] LIAO, S.Y., *"Microwave Devices and Circuits"*, Prentice-Hall Inc., Chapter 8-10, New Jersey, 1985

- [4] SANDER, K.F., *"Microwave Components and Systems"*, Chapter 4, Addison-Wesley, Bristol, 1987

- [5] DARYANANI, G.: *"Principles of Active Network Synthesis and Design"*, pp 287, John Wiley and Sons, New York, 1976

- [6] HOROWITZ and HILL, *"The Art of Electronics"*, pp 164, Cambridge University Press, 1980

- [7] CONNOR, F.R., "Antennas", Chapter 2, Edward Arnold Ltd, 1972
- [8] JULL, E.V. "Finite Range Gain of Sectional and Pyramidal Horns", Electronic letters, Vol 6, IEE Oct, 1970
- [9] OXLEY, T., "Microwave Solid State Devices", Chapter 14, New York, 1980
- [10] DUMAS, L.K., and SANDS, L.G., "Microwave System Planning", Chapter 4, Hayden Book Company, New York, 1967